DOI: https://doi.org/10.15446/ga.v23n2.89675

Integration of Geological, Mineralogical and Geochemical Methods in the Characterization of El Nitro and Las Alsacias Caves, Zapatoca (Colombia)

Integración de métodos geológicos, mineralógicos y geoquímicos en la caracterización de las cavernas El Nitro y Las Alsacias, Zapatoca (Colombia)

Diego Zafra-Otero[1], Carlos Alberto Ríos-Reyes[1]

ABSTRACT

The present study integrates geological, mineralogical and geochemical methods in the characterization of the caves: El Nitro and Las Alsacias, from Zapatoca (Colombia). With lithologies dating from the Lower Cretaceous, these cavities reveal a great variety of exokarst geoforms with different types of slips present on the surface, indicating changes in past atmospheric conditions. A great variety of speleothems (endokarstic geoforms) was also found, such as columns, stalactites, stalagmites, among others, which demonstrate a change in calcite saturation in the precipitated water. The morphology of the underground water bodies found showed variations in the dynamics of the karst aquifer (piezometric level and recharge), and it was evidenced that these cavities have structural control. The information obtained in the field (speleothematic catalogs, speleometry, maps, lithostratigraphy and structural data) were validated with atmospheric data and laboratory tests. This research provides new insights into geomorphology (epigeal and hypogeal), hydrogeology and mineralogy; serving as support for future work focused on paleoclimatic reconstruction, tectonic, paleosismic and climate change studies. These cavities represent scientific laboratories of great interest to the academy, since in them phenomena such as global warming and piezometric variations related to atmospheric phenomena can be evidenced.

KEYWORDS: geomorphology; karst; hydrogeology; petrography; cartography.

RESUMEN

El presente estudio integra métodos geológicos, mineralógicos y geoquímicos en la caracterización de las cavernas: El Nitro y Las Alsacias, de Zapatoca (Colombia). Con litologías que datan del Cretácico Inferior, estas cavidades revelan una gran variedad de geoformas exokársticas con diferentes tipos de lapiaces presentes en superficie, indicando cambios en las condiciones atmosféricas pasadas. Se encontró también una gran variedad de espeleotemas (geoformas endokársticas), tales como columnas, estalactitas, estalagmitas, entre otros, que demuestran un cambio en la saturación de calcita en el agua precipitada. La morfología de los cuerpos hídricos subterráneos encontrados demostró variaciones en la dinámica del acuífero kárstico (nivel piezométrico y recarga), y se evidenció que estas cavidades presentan un control estructural. La información obtenida en campo (catálogos espeleotemáticos, espeleometría, mapas, litoestratigrafía y datos estructurales) fueron validados con datos atmosféricos y pruebas de laboratorio. Esta investigación brinda nuevos conocimientos sobre geomorfología (epigea e hipogea), hidrogeología y mineralogía; sirviendo de apoyo a futuros trabajos enfocados a la reconstrucción paleoclimática, estudios tectónicos, paleosísmicos y de cambio climático. Estas cavidades representan laboratorios científicos de gran interés para la academia pues en ellas se pueden evidenciar fenómenos como el calentamiento global y variaciones piezométricas relacionadas a fenómenos atmosféricos.

PALABRAS CLAVE: geomorfología; karst; hidrogeología; petrografía; cartografía.

a Universidad Industrial de Santander, Grupo de Investigación en Geología Básica y Aplicada (GIGBA). Bucaramanga, Colombia. ORCID Zafra-Otero, D.: 0000-0001-5623-1180; ORCID Ríos-Reyes, C.A.: 0000-0003-0170-5558

b Correspondence author: dzafraotero@gmail.com

Reception: August 8, 2020. Acceptance: July 17, 2021

Introduction

Caves are underground systems (karst) representing one of the most outstanding geoforms on our planet. They are widespread all over the world in a variety of rock types and caused by several geological processes. However, they are not interconnected through large physiographic provinces, varying in shape and size from micro-fissures to several thousands of meters deep and high, and hundreds of kilometers in length (Lee et al., 2012). The scientific study of caves is called speleology, which is a multidisciplinary science in which geology, biology, hydrology and archaeology converge. Caves are underground environments with no natural light and present many obstacles, and cave explorers are who venture go through these obstacles, motivated by curiosity to discover and document places previously unknown (Kambesis, 2007). One of the most important activities developed during the systematic cave exploration are the cave mapping, which illustrate the extent and layout of the cave, shapes of passages (Kambesis, 2007) and help to establish the correlation between the surface above and the caves below, to compare caves to each other by length, depth and volume, to reveal important clues on the speleogenesis, to provide a spatial reference for future scientific work, and to assist tourist activities. The speleological maps not only show the geography of the caves, but also illustrate their different characteristics, which include the photography and description of speleothems.

For hundreds of thousands of years, the drops of rainwater that fall on the surface are beginning to open up mainly along fissures or fractures or through porous and permeable strata to reach the karstic cavities (e.g., Audra and Palmer, 2011), generating different types of speleothems (stalagmites, stalactites, and flowstones), which have become important climatic archives of continental climate variability and a novel area of paleoclimatic research (e.g., Mcdermott, 2004; Fairchild et al., 2006; Lachniet, 2009). Stalagmites, in particular are of great importance in paleoclimatic studies (e.g., Turgeon and Lundberg, 2001; Jones et al., 2018; Guo and Zhou, 2019) since they preserve an isotopic record of great importance to reconstruct the recent paleoclimatic history since they constitute a valuable archive on how the rain patterns have changed during the quaternary. They grow in protected enviroments that have often escaped to the radical alterations of the surface resulting from events such as glaciation, these interesting calcareous formations have become one of the most reliable archives for the understanding of past terrestrial climatic conditions due to their absolute chronologies, their continuous or semi-continuous deposition and their wide global distribution (e.g., Bradley 1999; Fairchild and Baker, 2012; Wong and Breecker, 2015; Denniston and Luetscher, 2017; Martín-Chivelet et al., 2017). They are amongst the most intensively explored archives of past climate change in continental settings, and the processes determining the internal structure of speleothems, such as mineralogy and crystal fabrics, are seldom used when interpreting speleothem geochemical proxies (e.g., Fairchild and Baker, 2012).

Paleoclimatic records from caves in speleothems can be related to changes in temperature, where they have proven useful in understanding global climate change (Fairchild et al., 2006). Speleothems have been used as climate indicators based on ^{234}U and ^{230}Th dating and $\delta^{18}O$ and $\delta^{13}C$ variations (e.g., Ayalon et al., 1999; McDermott, 2004; Fairchild and McMillan, 2007; Muñoz-Garcia et al., 2008; Railsback et al., 2017). Several analytical methods have been used in the characterization of speleothems, such as transmitted light microscopy (e.g., Ayalon et al., 1999; Jones, 2009; Fairchild and Baker, 2012; Perrin et al., 2014; Vanghi et al., 2015; Denniston and Luetscher, 2017), scanning electron microscopy (e.g., Jones, 2009; Vanghi et al., 2015; Denniston and Luetscher, 2017; Lima et al., 2019), electron microprobe analysis (e.g., Lima et al., 2019), computed tomography and magnetic resonance imaging (e.g., Zizu et al., 2012; Walczak et al., 2015; Wong and Breecker, 2015), micro-computed tomography (e.g., Vanghi et al., 2015; Du Preez et al., 2018), X-ray diffraction (e.g., Lima et al., 2019), micro X-ray fluorescence (e.g., Scroxton et al., 2018) or Raman, infrared, and Mössbauer spectroscopy (e.g., White, 2006; Gázquez et al., 2012; Lima et al., 2019). The internal speleothem microstratigraphy has taken relevance to facilitate uniform interpretations and

improve the geochemical and isotopic proxies (e.g., Turgeon and Lunberg, 2001; Muñoz-García et al., 2008, 2016; Railsback et al., 2017; Frisia, 2015).

Hydrogeological research methods for karst systems include isotopic tracers (e.g., Goldscheider et al., 2008), spring hydrograph analysis (e.g., Fiorillo, 2009; Li et al., 2016; Hosseini et al., 2017) and hydrochemical sampling (e.g., Moore et al., 2009; Rossi and Lozano, 2016; Zhang and Li, 2019). More recently, techniques such as numerical modelling (e.g., Ghasemizadeh et al., 2012; McCormack et al., 2017) and geophysics (e.g., Bechtel et al., 2007; McCormack et al., 2017) have grown in importance and capability.

Colombia has numerous cases of underground environments (karst´s) with more than a hundred caves that have been recorded, many of which have not been studied in detail. The Eastern Cordillera is one of the most important regions in terms of the geodiversity of karsts, mainly due to certain lithological and structural characteristics that have allowed to the formation and development of large underground systems (Muñoz-Saba et al., 2013). There is an interactive database on the kastic potential of Santander with updated information (Galvis, 2018), the explanation of which can be found in Galvis and Velandia (2019). In the Magdalena Middle Valley there are many limestone and other soluble rocks as the Rosablanca Formation (Lower Cretaceous), which is composed mainly of dolomitic limestones and evaporitic limestones with few intercalations of rocks of terrigenous origin in the lower part (Guzmán, 1985), within which karst environments have developed. Muñoz-Saba et al. (2013) report in the department of Santander more than 200 karstic manifestations with a great variety of caves associated mainly to the Rosablanca and Tablazo formations. The carbonate rocks that emerge in the municipality of Zapatoca have left with their presence a large number of karst geoforms that include: caves, dolines, karren, sinkholes, etc. The aims of this study are the geospeleologic description by means of geological, mineralogical and geochemical methods of the Nitro and Alsacias caves in Zapatoca (Colombia), and the microstratigraphic analysis of speleothems that could be the basis for the application of geochemical proxies for future climatic, paleontological, tectonic and biological studies.

Geological setting

The study area is located geographically in the vicinity of the municipality of Zapatoca. From the geological point of view, it forms part of the western region of the Santander Massif, Eastern Cordillera, Colombian Andes (Figure 1). In this region, sedimentary rocks of Jurassic to Late Cretaceous (Girón, Los Santos, Rosablanca and Paja formations) ages crop out. The geological unit of interest in the present study is the Rosablanca Formation, from which the Zapatoca karstic system was developed. This unit appears widely in the department of Santander and its type locality is located on the Sogamoso River 1 to 1.5 km from the town known as the Tablazo (Morales, 1958). According to Clavijo (1996), its thickness reported in the type locality is 450 m, which decreases significantly in the E and W edges of the northern sector of the Middle Magdalena Valley Basin (MMVB). Julivert (1958) reports in the "Mesas" and "Cuestas" region a thickness of 318 m. The Rosablanca Formation is a fossiliferous unit (predominantly of mollusks in diverse fragmentation states), very cemented, for that its appreciable hardness, with minor intercalations of marls, calcareous shales and a tendency to decrease the content and size of macro-fossils towards the ceiling (Morales et al., 1958); at its base it is composed of evaporitic limestone and dolomitic limestone layers with few intercalations of terrigenous rocks (Guzmán, 1985); the middle part consists of biomicrites, marls and pelites (Guerrero, 2002); at its top it is composed of brown to gray oolitic limestones with traces of heavy minerals (pyrite) (ANH, 2012). It is characterized by the presence of very different and rare speleothems (f Zapatoca and the Mesa de Los Santos, Bedoya and Hefer (2013), based on $^{87}Sr/^{86}Sr$ isotope values, assign to the Rosablanca Formation rocks a Valanginian - Lower Aptian age.

The study area belongs to the eastern sector of the Middle Magdalena Valley basin (an intracordilleran basin tilted towards the east, disturbed by some folds and faults, and characterized by structures

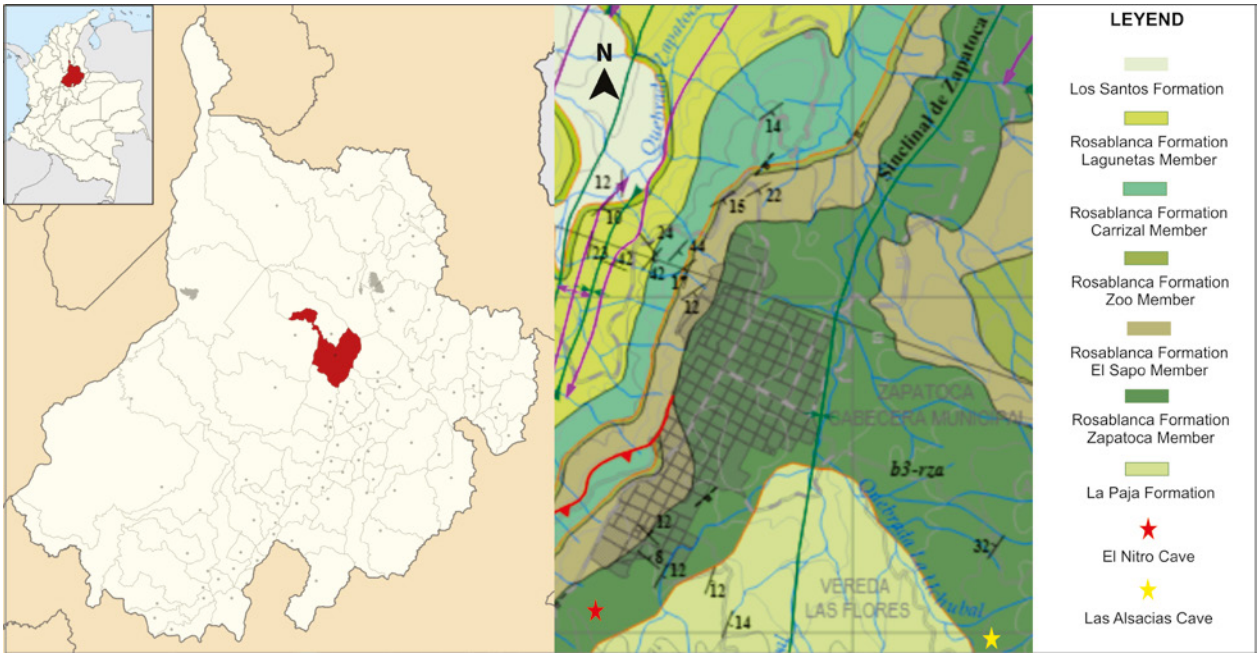

Figure 1. Geographical location of the study area, showing the El Nitro and Las Alsacias caves, adapted and modified after Etayo and Guzmán (2019)

with NE-SW direction). Structurally, this domain is defined by the reverse Suarez and Zapatoca faults with vergence to the east and the Los Cobardes Anticlinal and the Zapatoca Synclinal (Jiménez et al., 2016).

The hydrogeological characteristics of the El Nitro and Las Alsacias caves include geomorphological, geological, hydrological and geochemical aspects that we explain in this work, but that are not enough to understand the behaviour of these karst aquifers. However, the general knowledge of the karst hydrogeology summarized below is very important for those who are not familiar with the karst and with the differences in relation to the presence of underground aquifers (Taylor and Greene, 2008).

Materials and methods

Fieldwork

Fieldwork was developed between January and June 2019. Firstly, this included mapping and documenting the El Nitro and Las Alsacias caves. Information gathering was carried out on the cave's dimensions, finding known entrances, geology and geomorphology of the area, which was accompanied by the preparation of speleothematic catalogs, photographs of speleothems, structural data, tectonic evidences, and reconstruction of stratigraphic columns. A geomorphological map at a 1:20.000 scale of the exokarst present in the study area was carried out according to the methodology of Carvajal-Perico (2012).

Sampling of speleothems and water

Several samples from strategic points (fallen speleothems in active rooms with low sedimentation and rock samples from the inlets) were collected. They were already broken when collected, although it is unknown when or how this happened. Water sampling was carried out in both caves to determine pH, temperature (T) and total of dissolved solids (TDS).

Sample preparation

Three stalagmites were cut in half along their central growth axes using a Minosecar 2 ROWRATHENO diamond wet saw, and they were

then polished in a BUEHLER grinding-polishing machine.

Sample characterization

Polished sections were used to study the mineral composition and structure (textural and microstructural characteristics) of the stalagmite laminae by stereomicroscopy. Subsequently, the speleothem architectural analysis (SAA) was carried out according to Martín-Chivelet et al. (2017) as a stratigraphic procedure, through the analysis of architectural elements and sequential stratigraphy, used by geoscientists to categorize stratigraphic heterogeneities in sedimentary deposits. A microscopic analysis of the mineral composition, and textural and microstructural characteristics of the polished surfaces of stalagmites was performed using a FEI QUANTA 650 field emission gum environmental scanning electron microscope (FEG-ESEM), under the following analytical conditions: magnification = 100-20000x, WD = 9.0-11.0 mm, HV = 20 kV, signal = BSE in ZCONT mode, detector = BSED, EDS Detector EDAX APOLO X with resolution of 126.1 eV (in. Mn Kα). All the samples were carbon coated for their analysis. Temperature, pH, and total of dissolved solids of water were measured by a Pen type pH meter and acTDS meter 3 (water quality tester).

Data processing

The structural data were processed with the aid of the Stereo 32 program; rose diagrams were made to do a structural analysis of the geoforms, faults and fractures. The geomorphological map was made with the ARCGIS program.

Results

Karst

Exokarst

The dominant geomorphological environment in the area is the karst (Figure 2), but structural and denudative environments are also found (Zafra, 2019). The main geoforms found are: poljes, uvales, lapiaces fields, sinkholes, fault slopes, triangular facets, residual hills, remnant hills and a structural plateau. The entrance of El Nitro Cave is by means of a field of lapiaces of great depth while Las Alsacias Cave is entered by a chasm or trap.

In this study, several type of karren were identified, according to the classification proposed by Ginés (1990). This author classify karren as that formed by impacting, circulating, infiltrating or stagnant water, which were observed in the studied karstic system. The karren formed by impacting water includes the rillenkarren (striae and plains). Karren associated to circulating water includes wandkarren (wall channels), maanderkarren (meandering channels), trittkarren (steps) and cockling patterns (concavities). Karren associated to stagnant water corresponds to bucket or Kamenice and cavernous weathering. Karren formed by water that infiltrates is the rundkarren (rounded channels). All these types of karren can indicate climatic periods very varied in the region with intermittences between wet and dry periods as demonstrated by the variety of karren based on meteorological data provided by IDEAM (2020). The karren types are very important to know climatic events because they differ in their characteristics at different heights above sea level and that should be studied a depth in subsequent investigations.

Endokarst

In the studied caves, branching networks of conduits meander along fractures, fissures, and bedding planes, generating tributaries in the downstream direction, represents one of the most important characteristics of these karsts. Throughout the limestones of the Rosablanca Formation, several flow zones were developed along such planes of weakness. The enlarged openings in the limestones generated a groundwater flow, which produced further dissolution of these rocks, promoting the development of sinks and springs. There is no doubt that these karsts probably evolved as a result of hydrologic conditions, which changed significantly over geologic time.

In the El Nitro Cave, the following speleothems, mineralizations and underground geoforms are present. Parietal forms: Moonmilk, precipitation of malachite, karren endokarstic, calcite and

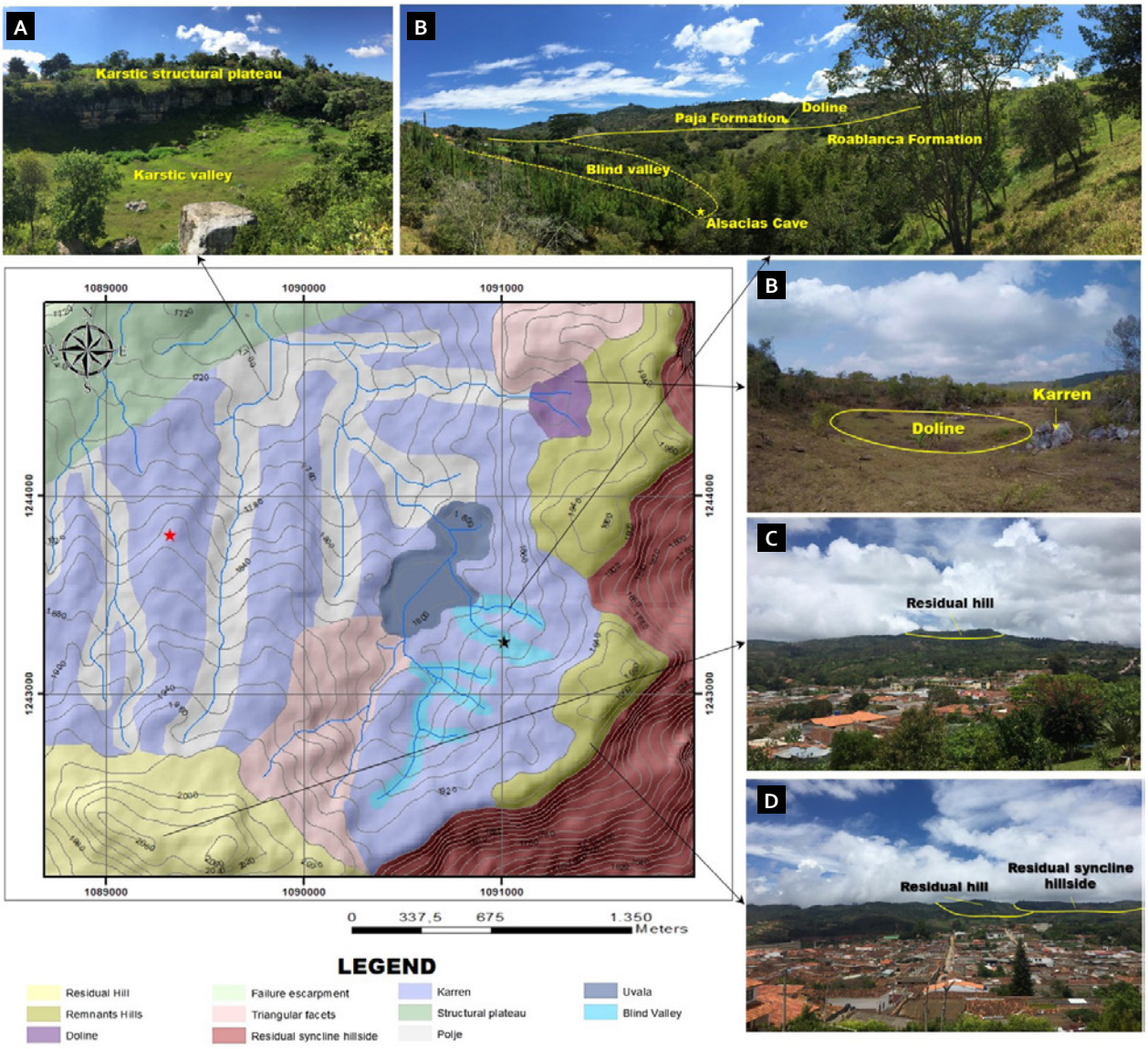

Figure 2. Geomorphological map of the study area illustrating its karstic geomorphology. The stars in red and black illustrate the geographical location of the El Nitro and Las Alsacias caves, respectively. Photographs illustrate several examples of the exokarstic features

aragonite crystals, plaster sheets, shelves, castings. Zenital forms: stalactites, elephant foot stalactites, sulfur precipitation, domes created by CO_2 emanated thanks to the breathing of bats. Pavementaries: Fried egg, flat base, botryoidal and popcorn stalagmites in fossilization and calcite rafts. Mixed: Columns, micro-columns and bathtubs. Fluvial geoforms: Siphons, wells and underground streams. The development of this cave is mostly horizontal with some vertical passages, the cave presents intermittent hydrological activity with small waterfalls of rainwater, speleothems of the "bathtub" type, wells and siphons; there are some sinks in the road with which we must be careful, we also observe the predominance of erosion over the dissolution, finally this cave has many features of periods of senility (sedimentation and fossilization phases) and maturity (clastic and stalagmitization phases) (Llopis, 1970).

In the Las Alsacias Cave, there is a very greatest diversity of speleothems. Zenital forms: Stalactites like soda straws, coraloid stalactites and flags. Parietal forms: Eccentric (helictites, antodites and

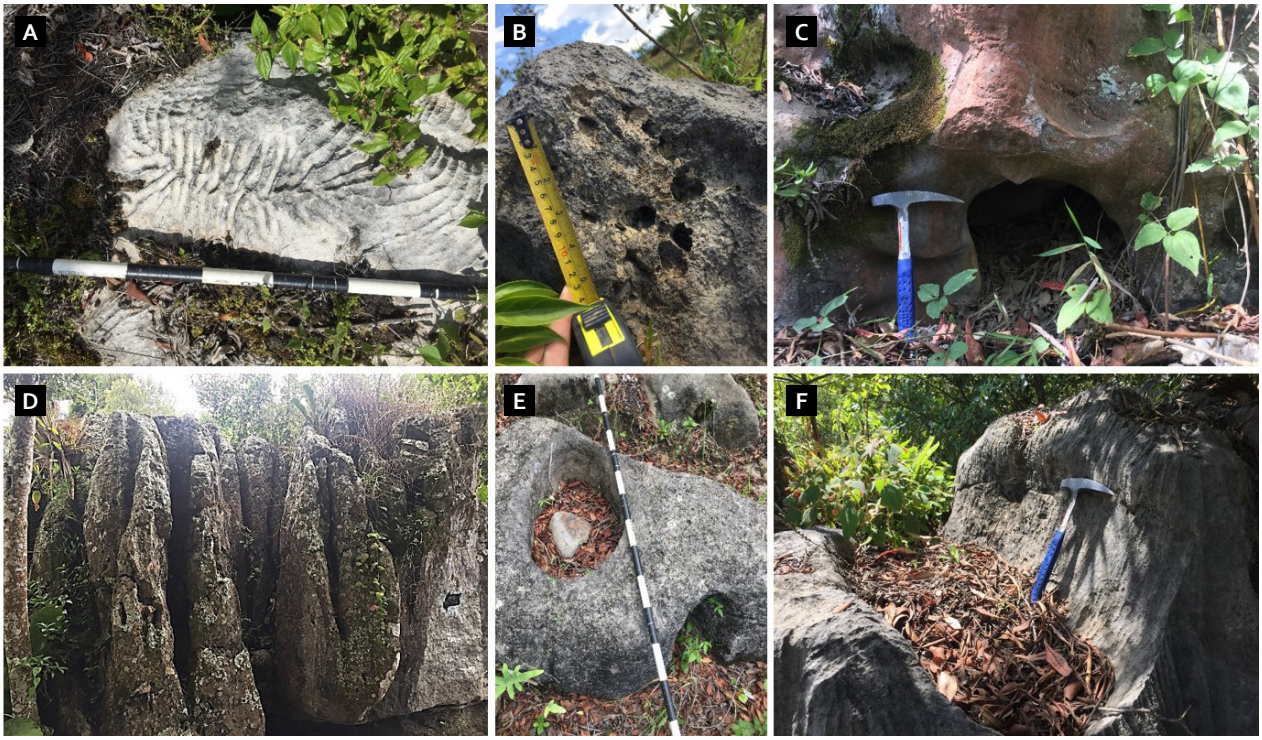

Figure 3. Examples of types of karren in the study area. (a) Rillenkarren. (b) Wandkarren. (c) Rainpits. (d) Kamenice. (e) Cavernous weathering. (f) Rundkarren

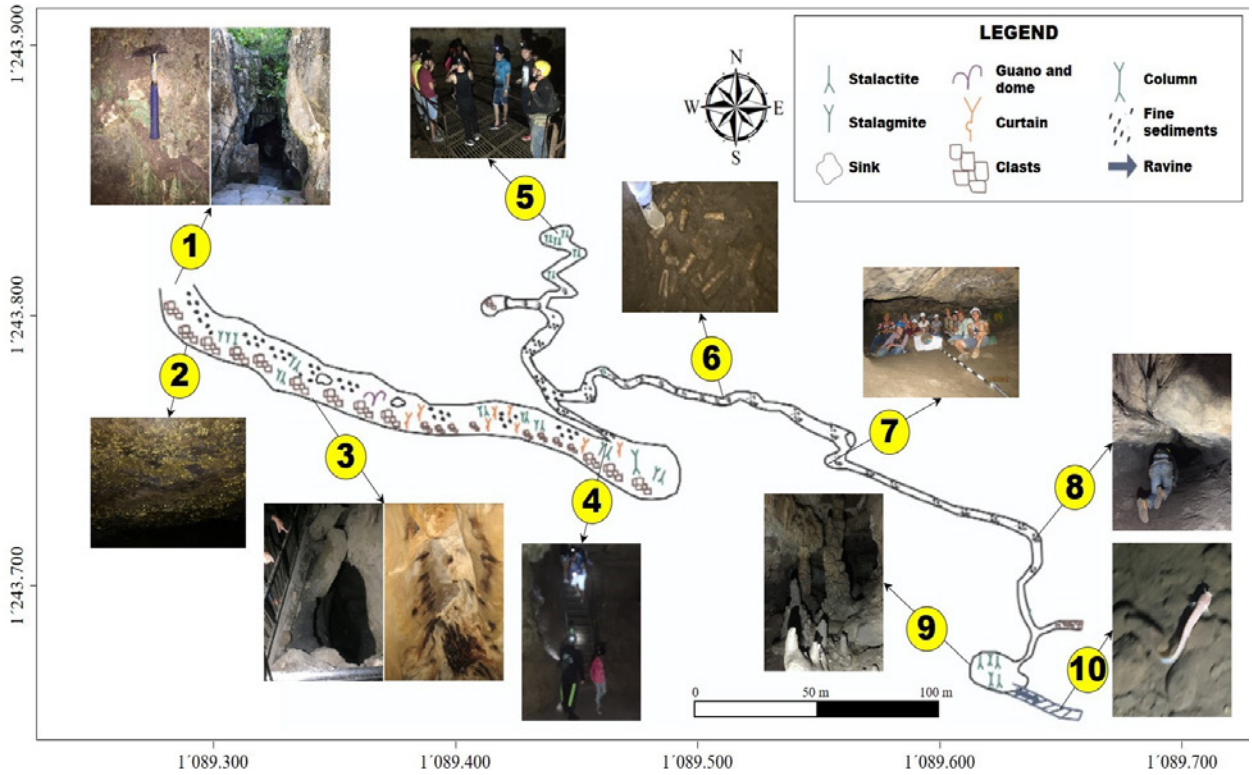

Figure 4. El Nitro Cave map. Route: 1, entry; 2, youth hall; 3, nun jump and bats lounge; 4, metal stairs; 5, platform; 6, tea room; 7, jump of the monkey; 8 tunnel of the 60m; 9, screw room; 10, stream of the blind fish

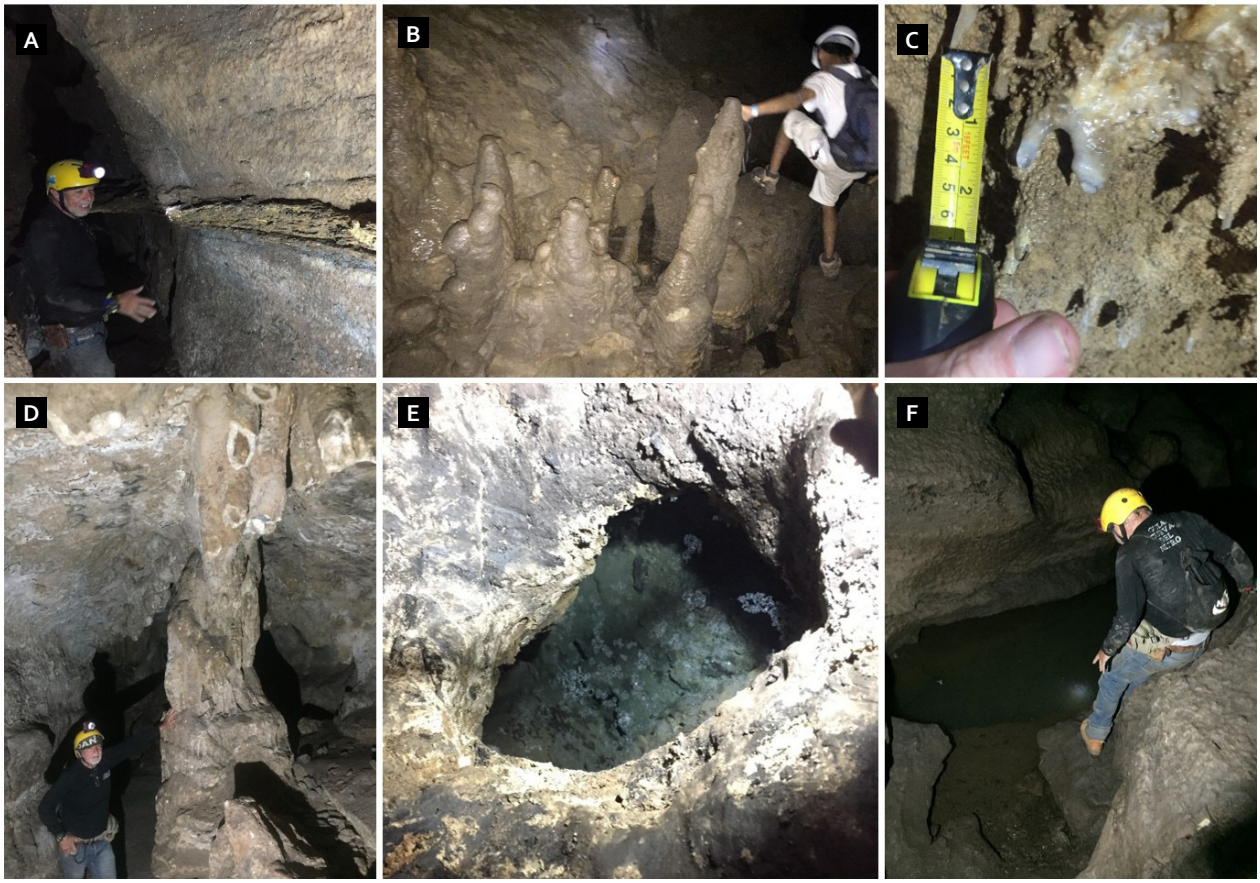

Figure 5. Endokarst in El Nitro Cave. (a) Ledge and sparite casting. (b) Column of 5 m. (c) Flat base stalagmites. (d) Well with calcite rafts. (e) Stalactite in the process of formation. (f) Siphon

anemolytes), saw teeth, plaster flowers, globular bark, moonmilk, sulfur precipitation and castings. Pavementaries: Stalagmites fried egg type, botryoidal and flat base, conulites, pearls of the caves and microgours. Mixed: Columns and flags. Fluvial Geoforms: Underground ravines, underground wells, paleochannels and paleobars of an underground paleo river that formed this system. The cave has constant water activity with low caudal and its development is mostly horizontal and sub horizontal.

Tectonics and palaeoseismic indicators

Cave speleothems can be used as tectonics and palaeoseismic indicators (Gilli, 2005). The study of El Nitro and Las Alsacias caves has allowed determining some evidences associated with faults, which have generated a change of direction and dip breaking of some speleothems as described below.

El Nitro Cave displays two faults (Figure 8, a-b), which reveals that this underground cavity has been subjected to extensional regimes during its most recent history: a strike-slip fault (N35°W/16°SW) is observed in the corridor adjacent to the entrance where there is a large column fractured and displaced in its upper part, and a fault with a strike of N60°W and a dip of 40°SW (Figure 8a) is observed in the spider room where there is a smaller column fractured and displaced. On the other hand, at least three large-scale paleoseismic events can be evidenced, the first one are the fossilized stalactites in the Salto del Mico, the second is the big column transported into the Blind Fish ravine and the last one is the inclined big stalagmite in the Hall of Screws. The fractures in this cave have a tendency characterized by a strike of N35°W and a dip of 80°SW.

Las Alsacias Cave shows a structural regime characterized by strike-slip (with sinistral movement,

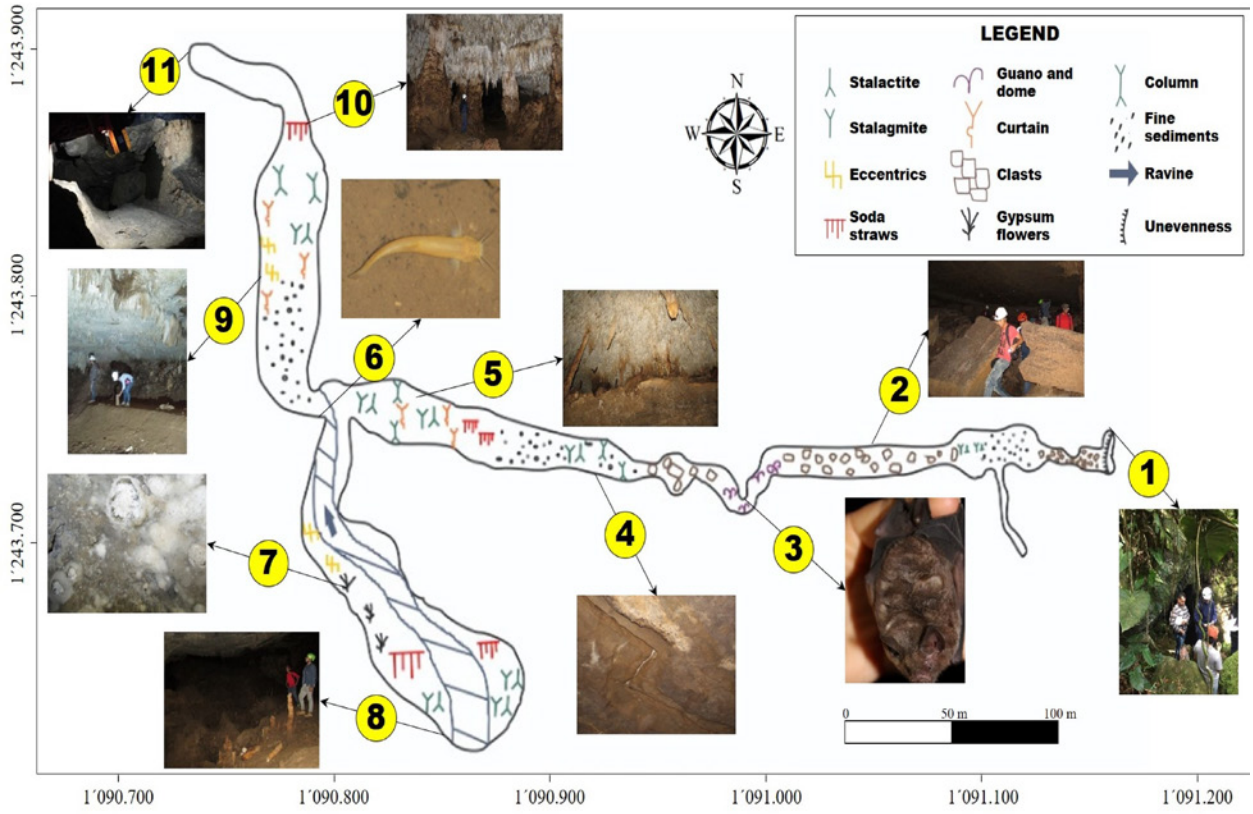

Figure 6. Las Alsacias Cave map. Route: 1, entry; 2, fallen blocks; 3, bats; 4, strait fault; 5, first castle; 6, gypsum flowers and eccentrics; 8, speleothems´s cemetery; 9, paleo river; 10, second castle; 11, wells

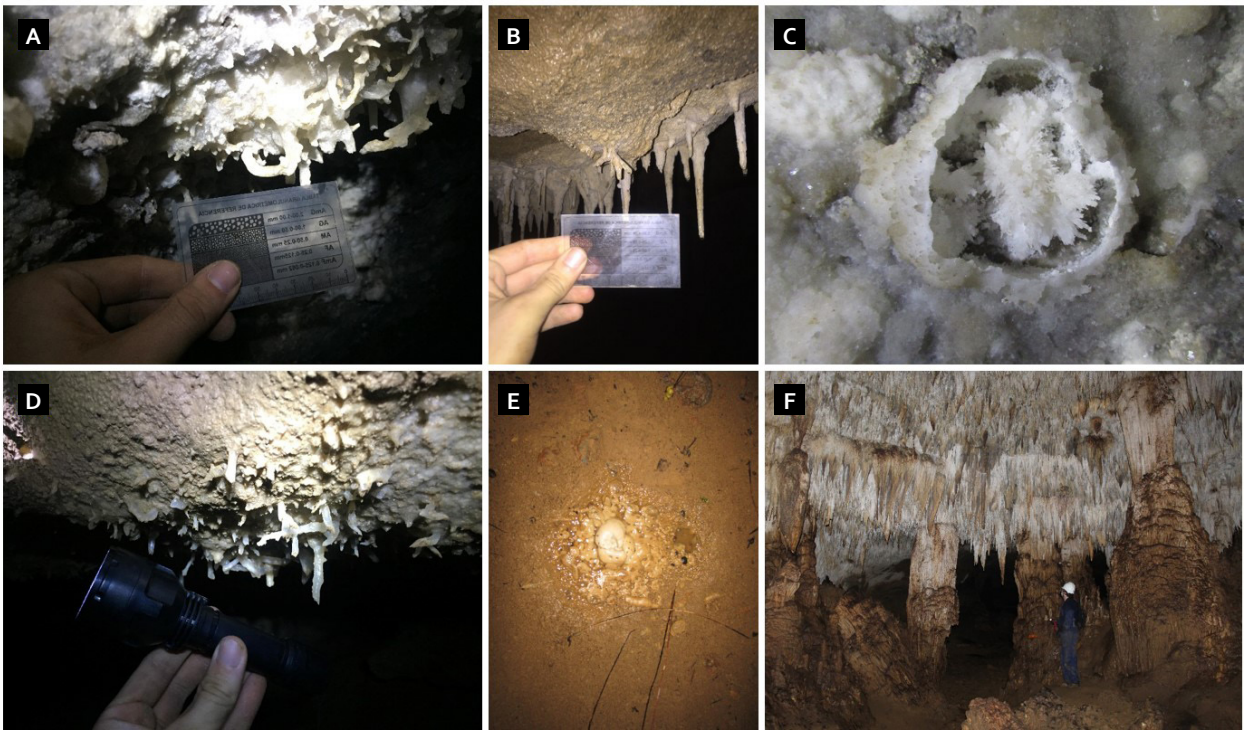

Figure 7. Endokarst in Las Alsacias Cave. (a) Eccentric type Antodite. (b) Eccentric Helictite type. (c) Eccentric type Anemolite. (d) Stalagmite in formation (Fried Egg Type) and Pisolite. (e) Gypsum flower. (f) Columns, stalactites, stalagmites, curtains and flags

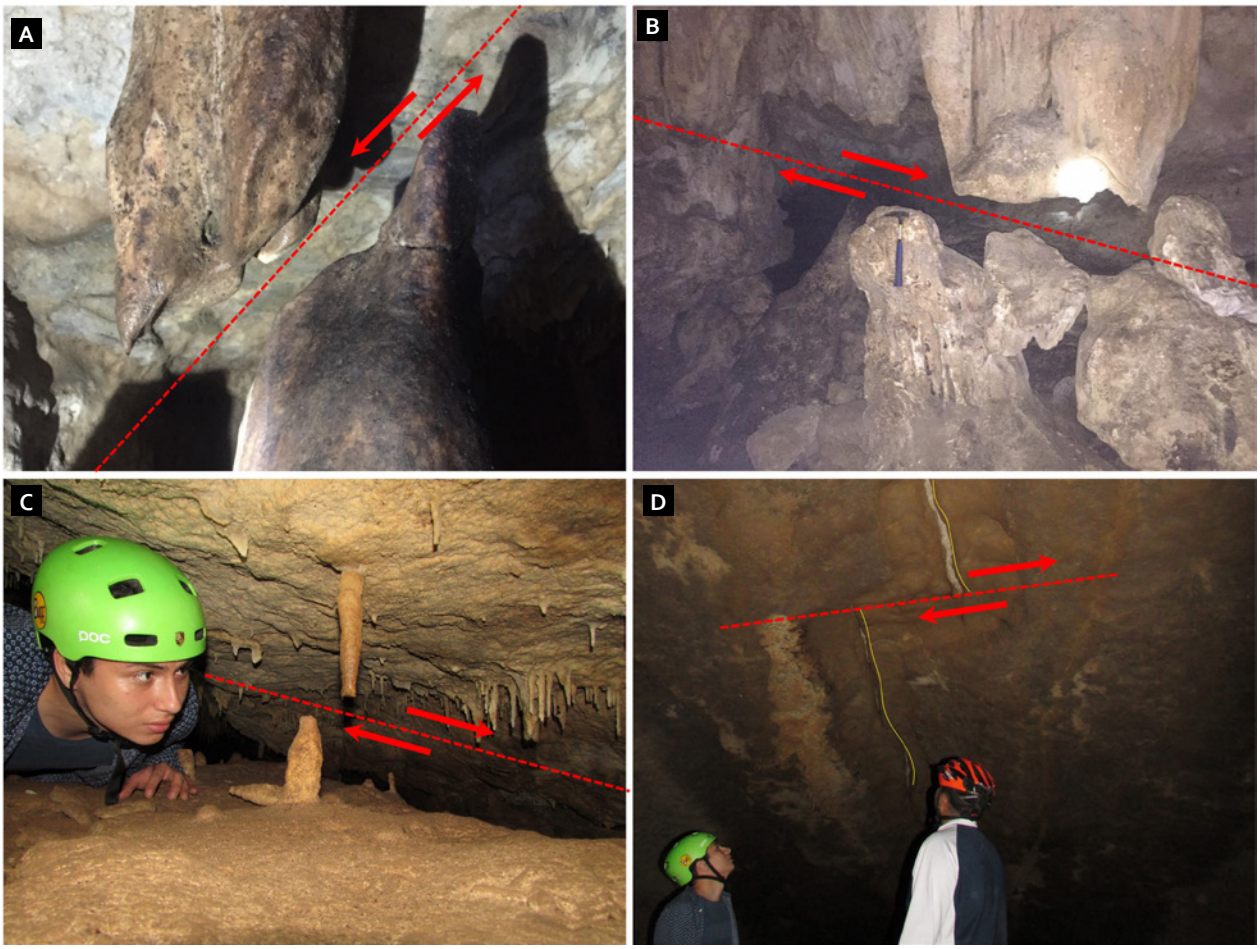

Figure 8. (a)-(b) Normal faults in El Nitro Cave. (c) Reverse and (d) strike-slip faults in Las Alsacias Cave

not measured) and inverse faults. The strike-slip fault is manifested in the roof of the cavity where a displacement of 74 cm of a fracture is observed. At least two reverse faults are observed on broken speleothems (columns), the first with a strike of N35°E and a dip of 45°NW, the other one have a strike of N45°W and a dip of 27°SW, respectively. On the other hand, there are at least three large-scale paleoseismic events, which are evidenced by: the twisted column of 3 m of height (first castle), the stalagmites fallen in the hall of the cemetery of speleothems and the stalagmites (fallen by tectonic movements) transported by the underground river. The fractures in this cave show a strike N15°W and a dip 80°NW or 80°SE.

The structural analysis based on the geomorphological map reveals the occurrence of poljes aligned in preferential directions of N4°E and N10°E, triangular facets aligned N37°E with the uvale and remaining hills, blind valleys mostly aligned with a strike N5°E, and that the caves are separated on the surface by a straight line of approximately 1.6 km distance. The analysis of poljes and blind valleys reveal that their strikes coincide with structural trends similar to each other.

A structural analysis of the cave maps was carried out, taking into account the route data of their galleries, halls and corridors, which were represented by means of the rose diagrams of the structural data of each cave were to make a comparison of them. The two rose diagrams made in the Stereo 32 program have similar shapes. The main trends of Las Alsacias and El Nitro caves are N70°W and N85°W, respectively, and, therefore, it can be seen that the two caves have a fairly similar stress regime, which differs by only 15° and so we consider that they have similar origins in geological time or even some internal connection since the end of these caves has never been found.

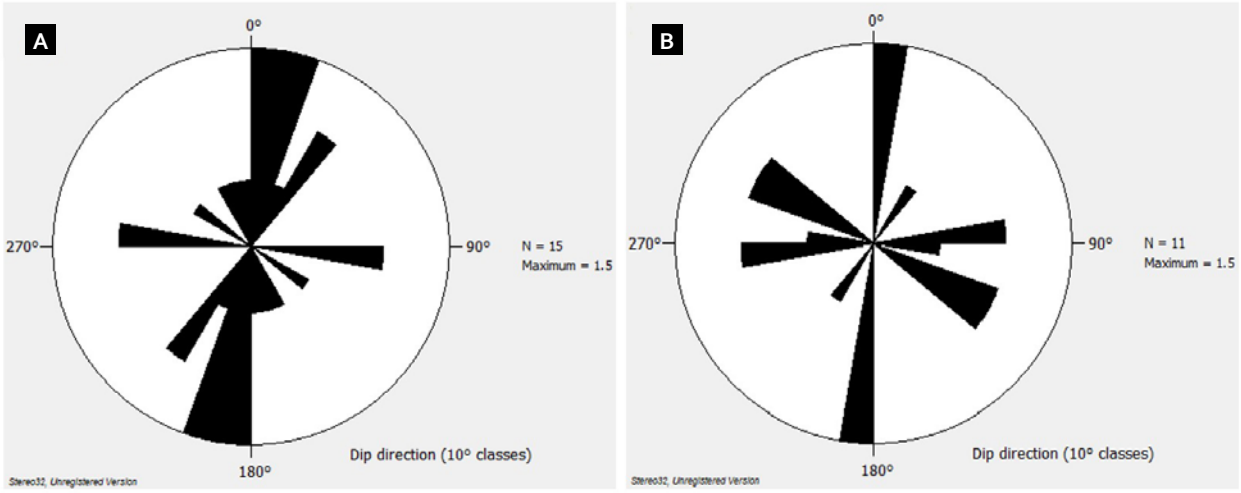

Figure 9. Structural analysis based on the geomorphological map (a) Rose diagram with the directions of the poljes, representing their alignment in the study area. (b) Rose diagram with the courses of the blind valleys, representing their structural alignment

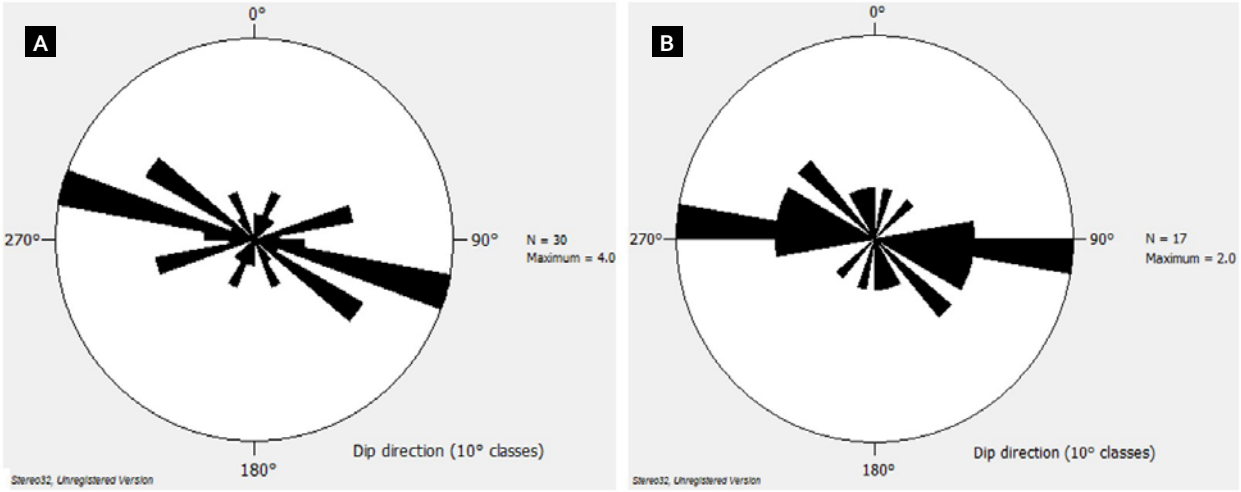

Figure 10. Structural analysis of the cavity´s galleries. (a) Rose diagram of El Nitro Cave. (b) Rose diagram of Las Alsacias Cave

Stratigraphy

Three stratigraphic columns of the Rosablanca Formation were made (Figure 11), corresponding to outcrops of rocks on the surface and from El Nitro and Las Alsacias caves, were documented in order to carry out their correlation. Column 1 (surface outcrop) is located on the road that goes from the municipality of Zapatoca to El Nitro Cave. It is just over 6 m in thickness and is composed mainly of calcareous sandstones; from base to top it consists of calcareous sandstones with highly bioturbated shells and mudstones with shells and bivalves (at the base), calcareous sandstones with bioturbated shells, some wackstones with shells and bivalves (in the middle part), and calcareous sandstones with shells and some mudstones with shells (at the top). The strata strike N30°W dipping more than 15°. It belongs to the Rosablanca Formation. Column 2 (El Nitro Cave) is approximately 11 m in thickness and is composed from base to top by wackstones with shells, bioturbated mudstones, calcareous sandstones with shells and high bioturbation, wackstones with bivalves, mudstones with shells, wackstones (separated by an erosive Surface, the upper with bivalves and the lower with shells), calcareous sandstones with high bioturbation and wackstones with

the presence of malachite and shells divided by erosive surfaces (the top contains bivalves). The strata strike N5°W dipping approximately 8°. It belongs to the Rosablanca Formation. Column 3 (Las Alsacias Cave) is approximately 14 m in thickness and is composed from base to top by calcareous sandstones with bivalves numaquelic grainstones and calcareous fissile mudstones with shells and gypsum crystals (at the base), mudstones with horizontal galleries, numaquelic grainstones and mudstones (in the middle part), wackstones with shells divided by an erosive surface and packstones with shells and bivalves (at the top). The strata strike N40-60°W dipping 15-40°. It belongs to the highest part of the Rosablanca Formation where the transitional contact with the Paja Formation begins to appear, which is evidenced by the layers of calcareous mudstones that emerge there.

Speleothem stratigraphy

According to Martín-Chivelet et al. (2017), the Speleothem Architectural Analysis (SAA) is based on the analysis of architectural elements and the stratigraphy of sequence. The SAA incorporates any petrographic or stratigraphic classification, being a useful, systematic and versatile method to unravel the complexities of the growth of speleothems and, therefore, to interpret genetically stalagmites on a multi-temporal scale. This analysis can also represent the basis for carrying out reconstruction of paleoclimatic series. In the present study some stalagmites from the El Nitro and Las Alsacias caves have been chosen to describe their stratigraphic stacking patterns (fourth order elements) in which they can be progressive, grade and retractive (Figure 12). The SAA in these speleothems was carried out

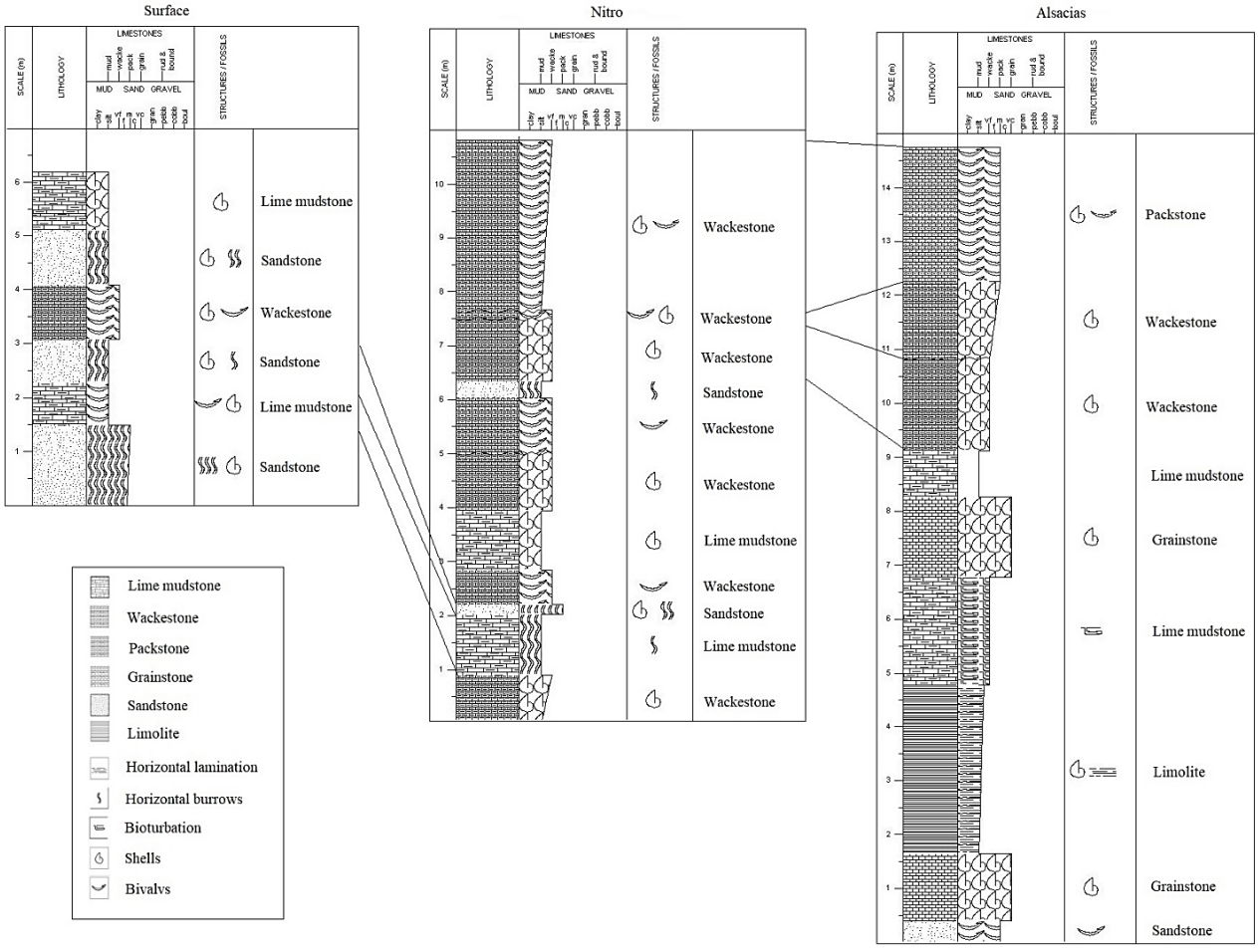

Figure 11. Stratigraphic columns of El Nitro and Las Alsacias caves and surface

in order to learn more about some climatic aspects of the area: knowing the paleorainfalls, the morphostratigraphy or the structure of the stalagmite lamination and thus understanding more about the paleoenvironments in which they were formed.

Stalagmite 1: comes from El Nitro Cave (Figure 12a). It is a speleothem that was recovered by the guides of this cave just before being sacked, the speleothem was donated by the guides for research. It belonged to the room of the screws and is the largest of those studied. It presents a large number of climatic events, to the naked eye it presents precipitated calcium carbonate with three different colorations due to different impurities in the precipitations: yellow (K), white (pure) and grayish (Fe). In the study, different growth patterns were also found, with the retractional and programmatic events being the most repeated, while the event with the greatest magnitude on the time scale was pleasant. Regarding the morphology of the lamination, it is of the globular type and of the subtype "bell shaped" or navel shape, this means that this stalagmite was formed with high and homogeneous drip cups, with low to moderate levels of calcite saturation.

Stalagmite 2: comes from Las Alsacias Cave (Figure 12b), specifically from the last room with speleothems of the upper gallery called the second castle. It shows two calcite compositions: the first one is white and the second one is grayish allowing to show different climatic events and compositions in the precipitation. We found different agradational, retractional and progradational growth patterns repeated in equal quantity, and a retrospective event that was the largest in the time scale. As for the morphostratigraphy of this stalagmite, it is observed that it begins with chaotic brain-type forms that indicate dry periods with high evaporation, then it begins to acquire frilled-type forms indicating lower drip cups and ends with globular forms.

Stalagmite 3: comes from Las Alsacias Cave (Figure 12c). It is quite crystalline and was collected in the hall of the fossil speleothems next to the underground ravine. It presents calcite of high purity, some yellowish colorations are observed and a quite marked hiatus, the most repeated growth patterns were the progradacionales and agrecionales, the event of greater magnitude in scale of time was progradational, a retractional event was found after the hiatus and more recent than the others. The morphoestratigraphy of this stalagmite is of the globular type match head, this represents high drip cups with increases in carbonate precipitation.

Franke (1965) demonstrated how the shapes of the stalagmites have variations due to the deposition process, proposing that a higher drip rate would cause an increase in the diameter of the stalagmites. Under stable conditions and constant growth over time, stalagmites grow in a balanced way (Dreybrodt and Romanov, 2008).

The studied stalagmites are 45.0, 10.5 y 7.5 cm long and 14.1, 4.0 and 2.5 cm wide, respectively. They are characterized by a columnar shape and growth that is approximately constant in diameter. In cross section, they display a typical layered nature with regular and visible layers (laminae) of dense calcite developing thin laminations, which cannot be considered as annual layers although they reflect changes in cave climate, surface conditions and other factors that may vary on decadal- to millennial-scales (e.g., Mariethoz et al., 2012).

Stalagmite laminae and growth surfaces were identified primarily on the basis of contrasts in colour. Shifts of growth axis are observed in several sectors. The stalagmite diameter does not show a substantial change towards the top. The axial parts of stalagmite 1 are encased by flanks of calcite-rich layers, which thin and pinch out downward, developing sharp boundaries (central horsts). In the case of stalagmites 2 and 3, these show very thin flanks of calcite-rich layers. The speleothem has three clearly defined petrographic segments with different crystal fabrics along its growth axis. According to Mcdermott et al. (2006), this type of growth pattern is attributed to a slow and low dripping rate, that are fed by vadose seepage flow water. The laminae of the stalagmite curve at the apex then thin and trail down the sides of the stalagmite; the curved morphology is interpreted to result from changes in the position of the drip location of the cave filtration of water over time (Al-Manmia et al., 2019). On the other hand, as seen in Figure 12, the growth direction had changed significantly with time as shown

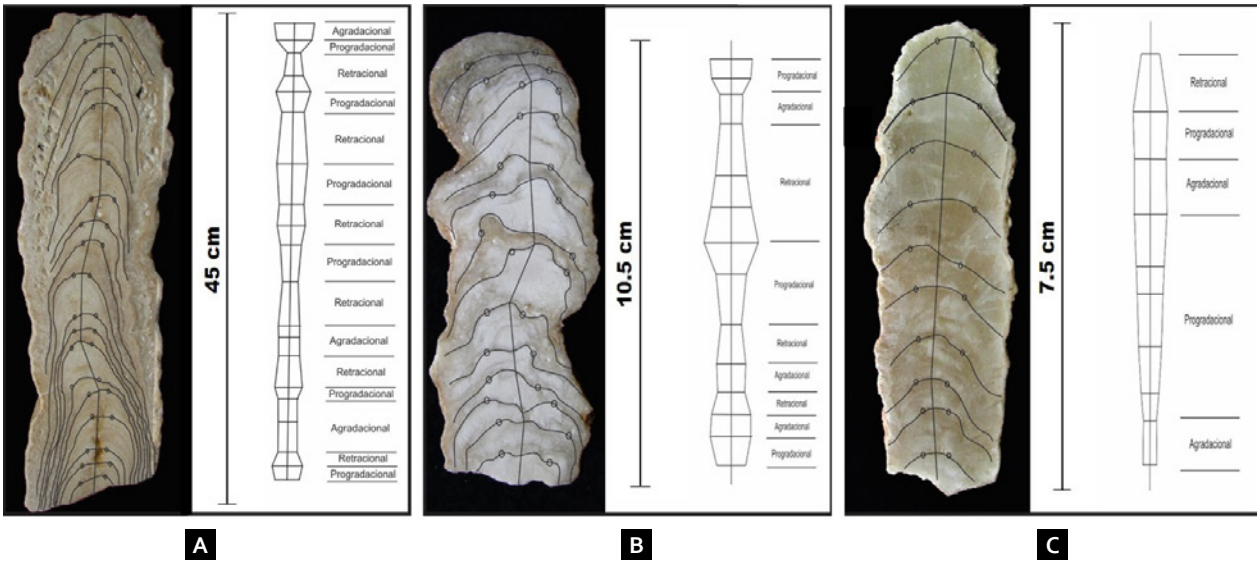

Figure 12. Fourth order architectural elements of (a) stalagmite from El Nitro Cave and (b)-(c) stalagmites from Las Alsacias Cave: Method for differentiating successive stacking patterns sets within a longitudinal polished section of a stalagmite, as proposed by Martín-Chivelet et al. (2017 p. 35): "In order to obtain quantitative logs, the distance between the "breakpoints" of each growth layer can be measured along the stalagmite. Variations in this distance through the growth axis allows defining trends and thus retractional, progradational or agradational sets"

by the distribution of the growth laminae. The studied stalagmites do not show hiatuses, suggesting continual growth.

SEM/EDS analyses

Scanning electron microscopy observations and elemental analysis by EDS of the analyzed speleothems showed a variety of crystalline mineral phases (Figure 13). Sample M1 (Figure 13a), belonging to the rock wall at the entrance of El Nitro Cave, corresponds to a limestone of biomicrite wackstone type with the presence of terrigenous, pyrite, iron oxides and malachite. Sample M2 (Figure 13b) corresponds to the rock wall at the entrance of Las Alsacias Cave, which is a limestone of biomicrite packstone type with terrigenous, iron oxides, potassium and calcium feldspars. Sample M3 (Figure 13c) belongs to crystalline parietal flowstones found in the diamonds room (El Nitro Cave); they are layered castings composed of calcite, aragonite and gypsum, with the presence of some zircons between the sheets. Sample M4 (Figure 13d) belongs to the same room from which stalagmite 2 was collected (last upper gallery room - second castle), and corresponds to a stalactite composed of calcite with different compositional impurities between its ducts, with rhodochrosite crystals as an accessory (for more data, see Annex 1).

Karst hydrogeology

The hydrogeological characteristics of both caves, although not studied in detail, reveal that the majority of halls of El Nitro cave are inactive, without flow and predominantly with sub horizontal development, and Las Alsacias cave is active with horizontal flow of water.

The two studied caves have hydric activity with horizontal and vertical water flows, in them it is possible to observe different hydrogeological manifestations that reveals evidences of the hydrodynamics of this karstic aquifer, such as: underground ravines, drip of speleothems, siphons, wells and waterfalls. These two underground systems should not be seen as isolated places from each other but as a large cave that is interconnected by means of fractures, the recharge zone of this aquifer is what can observe in the entrances and chasms of the cavities that present a mainly vertical and intermittent water flow, which depends mainly on atmospheric conditions. The two cavities have underground streams with constant flow (Alsacias) and intermittent (Nitro) that allow us to define the current piezometric level of

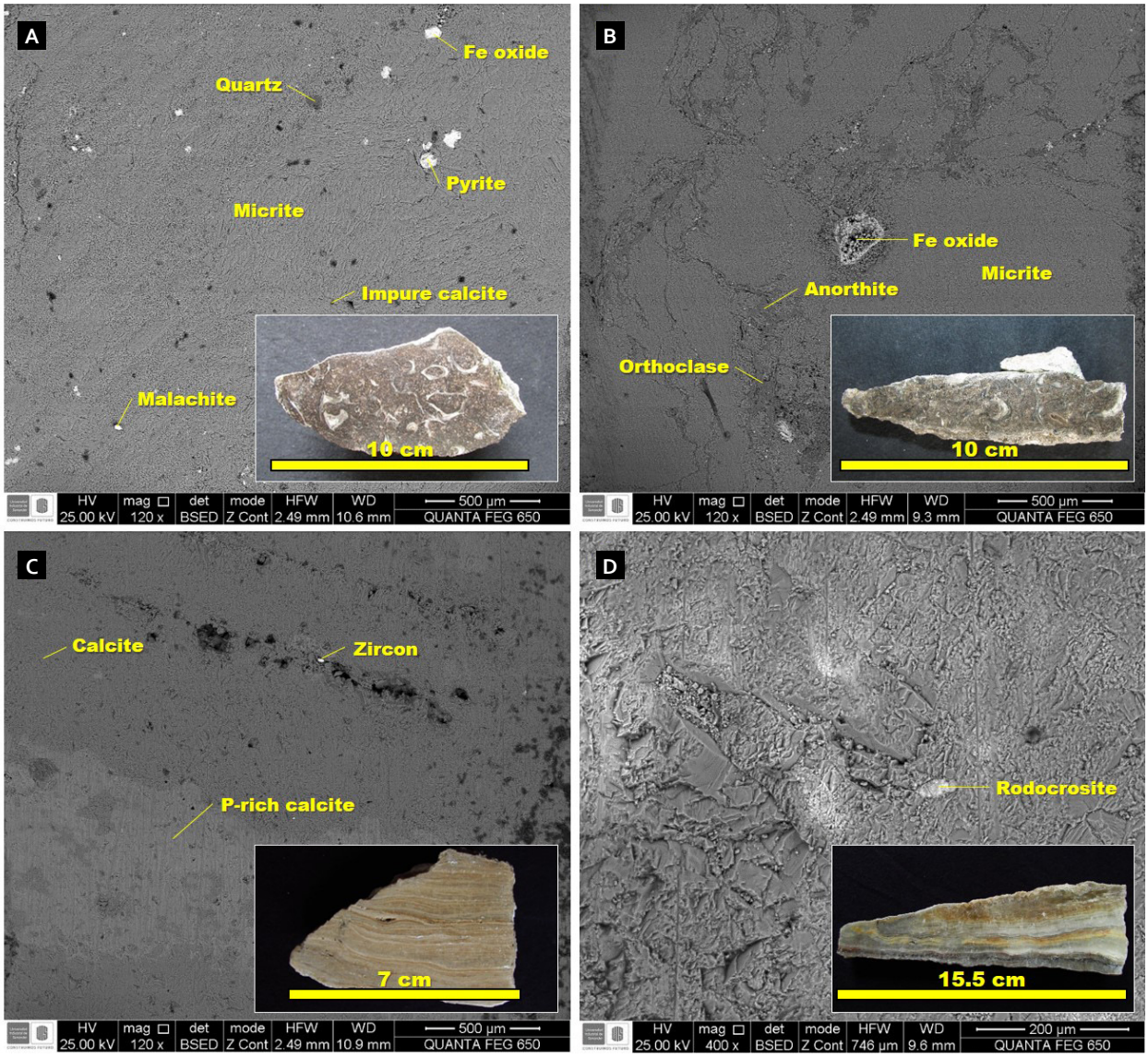

Figure 13. SEM/EDS analysis of speleothems from El Nitro and Las Alsacias caves. (a)-(b) Rock samples from El Nitro and Las Alsacias caves´ entrances, respectively. (c) Flooding from The Diamonds´s room (El Nitro Cave). (d) Stalactite from Las Alsacias Cave (for more data, see Annex 1)

the aquifer. The stagnant water in the cavities is due to increases and decreases in the piezometric level that are reflected in wells and siphons.

The flowing and stagnant water sources were analyzed to know their quality and to know if there was any source of contamination. El Nitro Cave: Stagnant water belonging to the room of the screws presented a PH of 8.1 (basic), TDS of 155 ppm and temperature of 22.5 °C. The water that flowed thanks to rainwater near the entrance showed a pH of 8.4 (basic), TDS of 244 and a temperature of 21 °C. Las Alsacias Cave: Stagnant water belongs to underground wells and presented a pH of 7.4 (basic), TDS of 188 ppm and temperature of 22.5 °C. The water that flowed belongs to the underground stream where the *Trychomycterus Sandovali* fish lives and presented a PH of 7.9 (basic), TDS of 158 ppm and temperature of 22.5 °C.

Discussion

During karst evolution, underground cavities are controlled not only by the initial structural settings of the rock, but also by the occurrence of fractures

represented by joints, faults, fissures, and bedding plane faults (Cooke et al., 1999) and the fluid flow conditions particularly within low porosity rocks (e.g., Klimchouk et al. 2000a; Brown, 2004; Bakun-Mazor et al., 2009; Agliardi et al., 2016).

The total annual rainfall and annual average temperature data acquired for the station of the Zapatoca stream from 1973 to 2015 (Figure 14) were provided by the information system of the Institute of Hydrology, Meteorology and Environmental Studies – IDEAM (2020), in order to know how recent climate change has been in this region and how this caves are affected, which is characterized by wet winters and dry summers. It was complemented with the information of the periods in which El Niño and La Niña phenomena were strong, recorded in the Pacific Ocean station of the IDEAM.

The climate in Zapatoca can be classified as tropical, with significant rainfall most months and short dry seasons; the average annual temperature is 18.8°C and the approximate average rainfall is 1735 mm. In Zapatoca, the highest temperatures are recorded between July and September, with a maximum daily average temperature greater than 21°C, with an average maximum temperature of 21°C and a minimum temperature average of 15°C, while the lowest temperatures are recorded between October and December, and the average daily maximum temperature is less than 20°C, with an average minimum temperature of 15°C and a maximum average temperature of 21°C. The rainfall in Zapatoca, expressed in average total accumulation, varies from 35 mm in January to 173 mm in October. Therefore, the hydrological years in this region have water deficit during the dry season (January) and significant infiltration during the wet season (October). On the other hand, during the rainy season, in conditions of low evaporation, infiltration to the caves increased, enhancing the drip discharge response to winter rainfall as suggested by Mahmud et al. (2018).

Figure 14 shows a decrease in rainfall and an increase in temperature over the years in Zapatoca, which also explain why the cave´s ravines have dried up and the phreatic level of the karstic aquifers has decreased, these can be evidenced to in the shelves that the aquifer have left in some galleries of the caves and in the paleochannels and paleobars of the underground paleoriver that nowadays is just a ravine. Thanks to this, the dissolution of limestones has been descending to lower galleries of the cavities

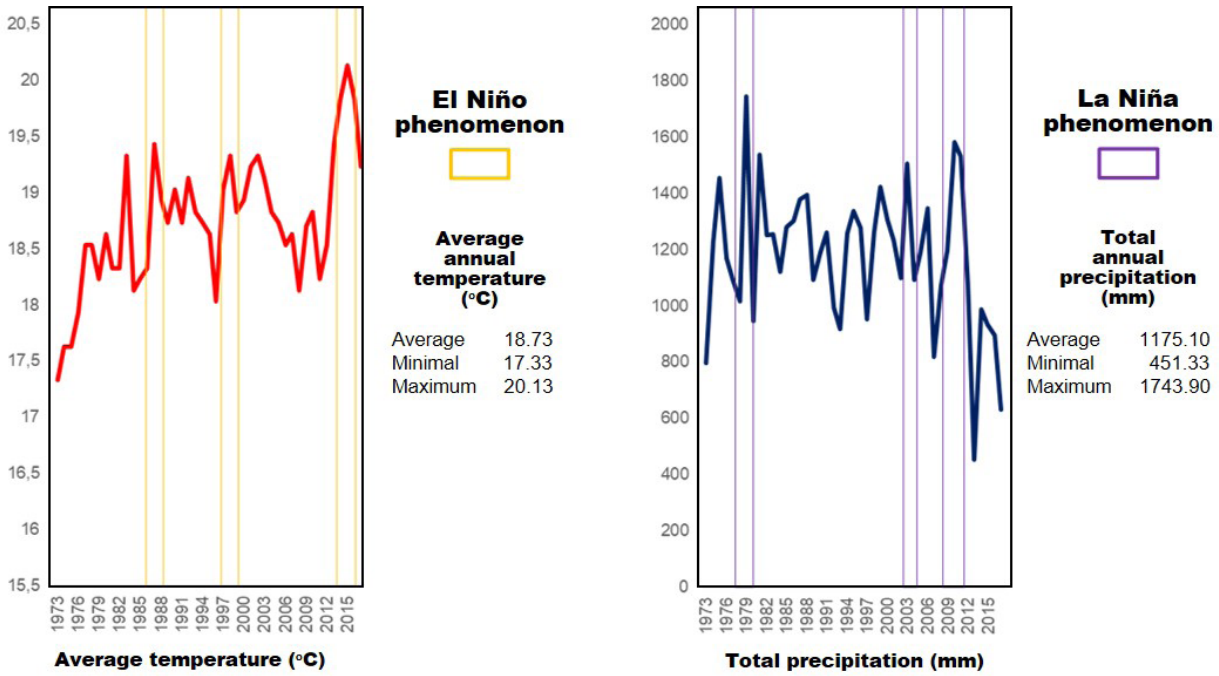

Figure 14. Climatology of the study area, average temperature and total precipitation since 1973 to 2015, with the periods in which La Niña and El Niño phenomena were more intense

where more water flows can be observed. The paleorainfalls recorded in the analyzed speleothems (Figure 12) coincide with the current climatic data since both demonstrate that Zapatoca has a bimodal climate with a fairly high dynamic.

The changing patterns of rainfall, when recharging groundwater in karstified regions, can be captured in speleothems via the hydrological behavior of the drip rates. Annually laminated stalagmites provide both a precise chronology and a paleoclimate proxy. The rate of annual vertical growth of stalagmites is recorded in changes of calcite fabric, annual fluxes of fluorescent organic matter or annual variations in trace element composition (e.g., Mariethoz et al., 2012). However, according to Duan et al. (2012), stalagmite laminae can be related to (1) fluorescent laminae formed by annual variations in organic matter flux (e.g., Proctor et al., 2000; Borsato et al., 2007; Hartland et al., 2014), (2) petrographic laminae formed by annual variations in calcite texture (e.g., Polyak and Asmerom, 2001; Martín-Chivelet et al., 2017), (3) calcite-aragonite couplets (e.g., Denniston et al., 2000), (4) trace-element laminae (e.g., Fairchild and Treble, 2009), and (5) aragonite laminae formed by the alternation of thin brown and thicker clear aragonite sub-layers (e.g., Yadava et al., 2004; Duan et al., 2010).

Changes in growth patterns of stalagmites provide valuable information on the paleoenvironmental conditions because their formation requires both H_2O and CO_2, which can reflect drip rates in the caves that depend on local precipitation and temperature conditions. According to Duan et al. (2012), the factors that control the growth rate of stalagmites are complex. During the summer, the relatively warm outside air and the relatively stable high pressures drive stagnant air into the cave with a high concentration of CO_2, while in winter, the caves are well ventilated as a result of the cold and dense outside air (with low atmospheric concentrations- CO_2 levels) displacing warmer, higher CO_2 content cave air (eg, Spötl et al., 2005; Banner et al., 2007). The factors that directly control the growth rate of a stalagmite are: the pH value and the drip rate, which are mainly controlled by the CO_2 concentration in the cave air and rainfall, respectively; However, the factor that most influences the growth rate is the concentration of Ca_2^+, which can be controlled by the local atmospheric temperature and rainfall (Duan et al., 2012).

A karst system is characterized as the result of a coupled mass-transfer/mass-transport process in soluble rocks with a permeability structure dominated by conduits dissolved from the rock and organized to facilitate the circulation of fluid, which depends on both, the aggressiveness of groundwater and its flow (e.g., Klimchouk et al., 2000b; Klimchouk, 2015). The groundwater flow is the main controller of the equilibrium/disequilibrium state in the fluid-rock interaction. Therefore, the speleogenesis process is developed by dissolution effects of disequilibria have to accumulate over sufficiently long periods of time and/or to concentrate within relatively small rock volumes or areas (Klimchouk 2015). The limestones of the Rosablanca Formation (the host of this caves) are soluble rocks with dense net of fractures, which have been enlarged by dissolution due to the flow of groundwater that promote an interaction fluid-rock, then karst conduits start to evolve developing a branch network of conduits probably with a dendritic pattern of flow, which formed these caves were so high, revealing that the rainy seasons on the past in this area were to much more longer and now the flows due to the reduction of the precipitation are lowest or they have been drying (dry up ravines), the vadose zone of these caves have left many wells due to the aquifer when the piezometric level raised up but nowadays the piezometric level does not raise up so much as the antique times generating that the cavities begin to dry. This study is the beginning to understand how the climate conditions of a zone affect a karst aquifer and how we can prove it with mineralogical studies and underground explorations, because of the aquifer has a dynamic behavior that depends on the rains in a zone (refill cup).

Conclusions

The studied karstification belongs to the Rosablanca Formation and the caves appear in the middle and upper part of this unit. El Nitro and Las Alsacias caves are governed by extensional and compressional regimes, respectively. The tunnels and

galleries in both caves have very similar course tendencies, which indicates that these two karstic systems are probably interconnected. A contribution to the mineralogy of speleothems and caves was made reporting for the first time in the area minerals like: rhodochrosite, malachite and zircons (indicating possible mineral deposits near this zone).

Paleorainfalls recorded in the speleothems indicate variations with a high dynamic where alternations are observed between dry, wet and stable periods of rains; the compositional changes of the speleothems layers indicate variation in the chemical emissions to the atmosphere.

The piezometric level of this aquifer has dropped because Zapatoca city has been affected by climate change since 40 years ago, indicating that the global warming is happening in this side of Colombia. The water in these caves is slightly basic, and the stagnant water has more neutral pH than the water that flows.

Conflict of interests: The manuscript was prepared and reviewed with the participation of the authors, who declare that there exists no conflict of interest that puts at risk the validity of the presented results.

References

Agencia Nacional de Hidrocarburos of Colombia (ANH), 2012. Cuenca Valle medio del Magdalena. Integración Geológica de la Digitalización y Análisis de Núcleos Pozo: Infantas-1613, Evaluación Petrofísica ShaleXpert Pozos: Catalina-1 y Cocuyo-1. Bogotá, DC.

Agliardi, F., Sapigni, M., and Crosta, G., 2016. Rock mass characterization by high-resolution sonic and GSI borehole logging. Rock Mech. Rock Eng. 49, 4303-4318. DOI: 10.1007/s00603-016-1025-x

Al-Manmia, D., Ismaeel, S., and Altaweel, M., 2019. Reconstruction of palaeoclimate in Shalaii Cave, SE of Sangaw, Kurdistan Province of Iraq. Palaeogeogr. Palaeoclimatol. Palaeoecol. 524, 262-272. DOI: 10.1016/j.palaeo.2019.03.044

Audra, P.,Palmer, A., 2011. The pattern of caves: Controls of epigenic speleogenesis. Géomorphol.: Relief Process. Environ. 17(4), 359-378. DOI: 10.4000/geomorphologie.9571

Ayalon, A., Bar-Matthews, M., Kaufman, A., 1999. Petrography, strontium, barium and uranium concentrations, and strontium and uranium isotope ratios in speleothems as palaeoclimatic proxies: Soreq Cave, Israel. Holocene 9(6), 715-722. DOI: 10.1191/095968399673664163

Bakun-Mazor, D., Hatzor, Y., Dershowitz, W., 2009. Modeling mechanical layering effects on stability of underground openings in jointed sedimentary rocks. Int. J. Rock Mech. Min. Sci. 46, 262-271. DOI: 10.1016/j.ijrmms.2008.04.001

Banner, J., Guilfoyle, A., James, E., Stern, L., Musgrove, M., 2007. Seasonal variations in modern speleothem calcite growth in Central Texas, USA. J. Sediment. Res. 77, 615-622. DOI: 10.2110/jsr.2007.065

Bechtel, Timothy Daniel, Bosch, Frank Peter, and Gurk, Marcus. 2007. Geophysical methods. In: Goldscheider, N., Drew, D. (Ed.), Methods in Karst hydrogeology. International Association of Hydrogeologists, London. pp. 171-200.

Bedoya, C., Hefer, N., 2013. Estratigrafía, quimioestratigrafía y petrografía de la formación Rosablanca: implicaciones para la identificación de eventos anóxicos oceánico en la Cordillera Oriental Colombiana. Undergraduate thesis, Universidad de Caldas, Manizales, Colombia.

Borsato, A., Frisia, S., Fairchild, I., Somogyi, A., Susini, J., 2007. Trace element distribution in annual stalagmite laminae mapped by micrometer-resolution X-ray fluorescence: Implications for incorporation of environmentally significant species. Geochimi. Cosmochim. Acta 71(6), 1494-1512. DOI: 10.1016/j.gca.2006.12.016

Bradley, R., 1999. Paleoclimatology. Reconstructing climates of the Quaternary. International Geophysics Series Vol. 68. Academic Press, Burlington, MA.

Brown, E., 2004. The mechanics of discontinua: Engineering in discontinuous rock masses. Aust. Geomech. J. 39(2) 1-20.

Carvajal-Perico, J., 2012 Propuesta de estandarización de la cartografía geomorfológica en Colombia. Instituto Colombiano de Geología y Minería (INGEOMINAS), Bogotá, DC.

Clavijo, J., 1996. Mapa Geológico de Colombia, Plancha 75. Aguachica, Escala 1:100.000. Memoria Explicativa. Instituto Colombiano de Geología y Minería (INGEOMINAS), Bucaramanga, Colombia

Cooke, M., Mollema, P., Pollard, D., Aydin, A., 1999. Interlayer slip and joint localization in East Kaibab Monocline, Utah: field evidence and results from numerical modeling. In: Cosgrove, J. Ameen, M. (Eds.), Forced folds and fracture. Geological Society of London, Special Publications. Vol. 169, London. pp. 23-49. DOI: 10.1144/GSL.SP.2000.169.01.03

Denniston, R., González, L., Asmerom, Y., Sharma, R., Reagan, M., 2000. Speleothem evidence for changes in Indian summer monsoon precipitation over the last ~2300 years. Quat. Res. 53(2), 196-202. DOI: 10.1006/qres.1999.2111

Denniston, R., Luetscher, M., 2017. Speleothems as high-resolution paleoflood archives. Quat. Sci. Rev. 170, 1-13. DOI: 10.1016/j.quascirev.2017.05.006

Dreybrodt, W., Romanov, D., 2008. Regular stalagmites: The theory behind their shape. Acta Carsologica 37(2), 175-184. DOI: 10.3986/ac.v37i2-3.145

Du Preez, G., du Plessis, A., de Beer, D., Forti, P., 2018. Non-destructive, high-resolution X-ray micro-CT of a Hairy Stalagmite: investigating the structural details of a biogenic speleothem. Int. J. Environ. Sci. Technol. 15, 1843-1850. DOI: 10.1007/s13762-017-1543-4

Duan, W., Cai, B., Tan, M., Liu, H., Zhang, Y., 2012. The growth mechanism of the aragonitic stalagmite laminae from Yunnan Xianren Cave, SW China revealed by cave monitoring. Boreas 41(1), 113-123. DOI: 10.1111/j.1502-3885.2011.00226.x

Duan, W., Tan, M., Cheng, H., Zhang, Y., 2010. Intra-annual structure of aragonitic stalagmite laminae from Yunnan Xianren Cave: SEM. Quat. Sci. 30, 1066-1067.

Etayo Serna, F., Guzmán Ospitia, G., 2019. Formación Rosa Blanca: subdivision de la Formación y propuesta de Neoestratotipo. Sección laguna El Sapo, vereda El Carrizal, municipio de Zapatoca, departamento de Santander. In: Estudios geológicos y paleontológicos sobre el Cretácico en la región del embalse del río Sogamoso, Valle Medio del Magdalena. Compilación de los Estudios Geológicos Oficiales en Colombia. Vol. 23. Servicio Geológico Colombiano, Bogotá, DC.

Fairchild, I., Baker, A., 2012. Speleothem science: From process to past environments. Wiley-Blackwell, Chichester, UK. DOI: 10.1002/9781444361094

Fairchild, I. McMillan, E., 2007. Speleothems as indicators of wet and dry periods. Int. J. Speleol. 36(2), 69-74. DOI: 10.5038/1827-806X.36.2.2

Fairchild, I., Smith, C., Baker, A., Fuller, L., Spötl, C., Mattey, D., McDermott, F., 2006. Modification and preservation of environmental signals in speleothems. Earth-Sci. Rev. 75, 105-153. DOI: 10.1016/j.earscirev.2005.08.003

Fairchild, I., Treble, P., 2009. Trace elements in speleothems as recorders of environmental change. Quat. Sci. Rev. 28(5-6): 449-468. DOI: 10.1016/j.quascirev.2008.11.007

Fiorillo, F., 2009. Spring hydrographs as indicators of droughts in a karst environment. J. Hydrol. 373(3-4), 290-301. DOI: 10.1016/j.jhydrol.2009.04.034

Franke, H., 1965. The theory behind stalagmite shapes. Stud. Speleol. 1, 89-95.

Frisia, S., 2015. Microstratigraphic logging of calcite fabrics in speleothems as tool for palaeoclimate studies. Int. J. Speleol. 44(1), 1-16. DOI: 10.5038/1827-806X.44.1.1

Galvis, M., Velandia, F., 2019. Mapa del potencial kárstico del departamento de Santander, Colombia. Revista de Topografía AZIMUT (10), 1-6.

Galvis-Gómez, M., 2018. Mapa del potencial kárstico del departamento de Santander (Colombia). Monographic thesis. Universidad Militar Nueva Granada, Bogotá , DC.

Gázquez, F., Calaforra, J. Forti, P., Rull, F., Martínez-Frías, J., 2012. Gypsum-carbonate speleothems from Cueva de las Espadas (Naica mine, Mexico): mineralogy and palaeohydrogeological implications. Int. J. Speleol. 41(2), 211-220. DOI: 10.5038/1827-806X.41.2.8

Ghasemizadeh, R., Hellweger, F., Butscher, C., Padilla, I., Vesper, D., Field, M., Alshawabkeh, A., 2012. Groundwater flow and transport modeling of karst aquifers, with particular reference to the North Coast Limestone aquifer system of Puerto Rico. Hydrogeol. J. 20, 1441-1461. DOI: 10.1007/s10040-012-0897-4

Gilli, E., 2005. Review on the use of natural cave speleothems as palaeoseismic or neotectonics indicators. Comptes Rendus Geosciences 337(13), 1208-1215. DOI: 10.1016/j.crte.2005.05.008

Ginés, A., 1990. Utilización de las morfologías de lapiaz como geoindicadores ecológicos en la Serra de Tramuntana (Mallorca). Endins 16, 27-39.

Goldscheider, N., Meiman, J., Pronk, M., Smart, C., 2008. Tracer tests in karst hydrogeology and speleology. Int. J. Speleol. 37, 27-40. DOI: 10.5038/1827-806X.37.1.3

Guerrero, J., 2002. A proposal on the classification of system tracts: Application of allostratigraphy and sequence stratigraphy of the Cretaceous Colombian Basin. Part 1: Berrisian to Hauterivian. Geologia Colombiana 27, 3-25.

Guo, W., Zhou, C., 2019. Patterns and controls of disequilibrium isotope effects in speleothems: Insights from an isotope-enabled diffusion-reaction model and implications for quantitative thermometry. Geochimi. Cosmochimi. Acta 267, 196-226. DOI: 10.1016/j.gca.2019.07.028

Guzmán, G., 1985. Los grifeidos infracretácicos *Aetostreon couloni* y *Ceratostreon boussingaulti*, de la Formación Rosablanca, como indicadores de oscilaciones marinas. Publ. Geolog. Esp. 16. Instituto Colombiano de Geología y Minería (INGEOMINAS), Bogota. pp. 1-16

Hartland, A., Fairchild, I., Müller, W., Dominguez-Villar, D., 2014. Preservation of NOM-metal complexes in a modern hyperalkaline stalagmite: Implications for speleothem trace element geochemistry. Geochimi. Cosmochimi. Acta 128, 29-43. DOI: 10.1016/j.gca.2013.12.005

Hosseini, S., Ataie-Ashtiani, B., Simmons, Craig., 2017. Spring hydrograph simulation of karstic aquifers: Impacts of variable recharge area, intermediate storage and memory effects. J. Hydrol. 552, 225-240. DOI: 10.1016/j.jhydrol.2017.06.018

Instituto de Hidrología, Meteorología y Estudios Ambientales of Colombia (IDEAM), 2020. Datos Meteorológicos Zapatoca (Santander) - Colombia. Available at http://dhime.ideam.gov.co/atencionciudadano/

Jiménez, G., López, O., Jaimes, L., Mier, R., 2016. Variaciones en el estilo estructural relacionado con anisotropías de basamento en el Valle Medio del Magdalena. Rev. Acad. Colomb. Cienc. Ex. Fis. Nat. 40 (155), 312-319. DOI: 10.18257/raccefyn.293

Jones, B., 2009. Phosphatic precipitates associated with actinomycetes in speleothems from Grand Cayman, British West Indies. Sediment. Geol. 219, 302-317. DOI: 10.1016/j.sedgeo.2009.05.020

Jones, B., Zheng, E., Li, L., 2018. Growth and development of notch speleothems from Cayman Brac, British West Indies: Response to variable climatic conditions over the last 125,000 years. Sediment. Geol. 373, 210-227. DOI: 10.1016/j.sedgeo.2018.06.005

Julivert, M., 1958. La morfoestructura de la zona de mesas al SW de Bucaramanga. Boletín de Geología 1, 7-44.

Kambesis, P., 2007. The importance of cave exploration to scientific research. J. Cave Karst Stud. 69(1), 46-58.

Klimchouk, A., Ford, D., Palmer, A., Dreybrodt, W., 2000a. Lithologic and structural controls of dissolutional cave development. In: Klimchouk, A., Ford, D., Palmer, A., Dreybrodt, W. (Eds.), Speleogenesis. evolution of karst aquifers. National Speleological Society, Huntsville, AL. pp. 54-64.

Klimchouk, A., Ford, D., Palmer, A., Dreybrodt, W. (Eds.), 2000b. Speleogenesis, evolution of karst aquifers. National Speleological Society, Huntsville, AL.

Klimchouk, A., 2015. The karst paradigm: Changes, trends and perspectives. Acta Carsologica 44(3), 289-313. DOI: 10.3986/ac.v44i3.2996

Lachniet, M., 2009. Climatic and environmental controls on speleothem oxygen-isotope values. Quat. Sci. Rev. 28, 412-432. DOI: 10.1016/j.quascirev.2008.10.021

Lee, N., Meisinger, D., Aubrecht, R., Kovacik, L., Saiz-Jimenez, C., Baskar, R., Liebl, W., Porter, M., Engel, A., 2012. Caves and karst environments. In: Bell, E., Callaghan, T. (Eds.), Life at extremes: environments, organisms and strategies for survival. CAB International, Wallingford, UK. pp. 320-344. DOI: 10.1079/9781845938147.0320

Li, G., Goldscheider, N., Field, M., 2016. Modeling karst spring hydrograph recession based on head drop at sinkholes. J. Hydrol. 542, 820-827. DOI: 10.1016/j.jhydrol.2016.09.052

Lima Figueira, R., Coimbra Horbe, A., Herrera Aragón, F., Freitas Gonçalves, D., 2019. Exotic sulphate and phosphate speleothems in caves from eastern Amazonia (Carajás, Brazil): Crystallographic and chemical insights. J. S. Am. Earth Sci. 90, 412-422. DOI: 10.1016/j.jsames.2018.12.007

Llopis, N., 1970. Fundamentos de la hidrogeología kárstica: Introducción a la geoespeleología. Blume, Madrid.

Mahmud, K., Mariethoz, G., Baker, A. Treble, P., 2018. Hydrological characterization of cave drip waters in a porous limestone: Golgotha Cave, Western Australia. Hydrol. Earth Syst. Sci. 22, 977-988. DOI: 10.5194/hess-22-977-2018

Mariethoz, G., Kelly, B., Baker, A., 2012. Quantifying the value of laminated stalagmites for paleoclimate reconstructions. Geophys. Res. Lett. 39, L05407. DOI: 10.1029/2012GL050986

Martín-Chivelet, J., Muñoz-García, B., Cruz, J., Ortega, A., Turrero, M., 2017. Speleothem architectural analysis: Integrated approach for stalagmite-based paleoclimate research. Sediment. Geol. 353, 28-45. DOI: 10.1016/j.sedgeo.2017.03.003

McCormack, T., O'Connell, Y., Daly, E., Gill, L., Henry, T., Perriquet, M., 2017. Characterisation of karst hydrogeology in Western Ireland using geophysical and hydraulic modelling techniques. J. Hydrol.: Reg. Stud. 10, 1-17. DOI: 10.1016/j.ejrh.2016.12.083

McDermott, F., 2004. Palaeo-climate reconstruction from stable isotope variations in speleothems: a review. Quat. Sci. Rev. 23, 901-918. DOI: 10.1016/j.quascirev.2003.06.021

McDermott, F., Schwarcz, H., Rowe, P., 2006. Isotopes in speleothems. In: Leng, M. (Eds.), Isotopes in paleoenvironmental research. Springer, Heidelberg, Germany. pp. 186-226.

Mendoza-Parada, J., Moreno-Murillo, J., Rodríguez-Orjuela, G., 2009. El sistema cárstico de la formación Rosablanca Cretácico inferior, en la provincia santandereana de Vélez, Colombia. Geología Colombiana 34, 35-44.

Moore, P., Martin, J., Screaton, E., 2009. Geochemical and statistical evidence of recharge, mixing, and controls on spring discharge in an eogenetic karst aquifer. J. Hydrol. 373(3-4), 443-455. DOI: 10.1016/j.jhydrol.2009.07.052

Morales, J., 1958. General geology and oil ocurrences of Middle Magdalena Valley, Colombia. AAPG Habitat of Oil Symposium A125, 641-695.

Muñoz-García, M., Cruz, J., Martín-Chivelet, J., Ortega, A., Turrero, M., López-Elorza, M., 2016. Comparison of speleothem fabrics and microstratigraphic stacking patterns in calcite stalagmites as indicators of paleoenvironmental change. Quat. Int. 407A, 74-85. DOI: 10.1016/j.quaint.2016.02.036

Muñoz-García, M., Martín-Chivelet, J., Rossi, C., Ford, D., Schwarcz, H., 2008. Comparación del clima

interglacial eemiense y holoceno en el norte de España a partir de los indicadores paleoclimáticos de estalagmitas de la Cueva del Cobre Palencia. Geo-Temas 10, 1459-1462.

Muñoz-Saba, Y., Casallas-Pabón, M., Murcia-López, D., Hoyos-Rodríguez, M., Rodríguez-Orjuela, G., Moreno-Murillo, J., Mendoza-Parada, J., 2013. Cavernas de Santander, Colombia. Serie de Guías: Instituto de Ciencias Naturales, Facultad de Ciencias, Universidad Nacional de Colombia, Bogotá, DC.

Perrin, C., Prestimonaco, L., Servelle, G., Tilhac, R., Maury, M., Cabrol, P., 2014. Aragonite-calcite speleothems: Identifying original and diagenetic features. J. Sediment. Res. 84, 245-269. DOI: 10.2110/jsr.2014.17

Polyak, V., Asmerom, Y., 2001. Late Holocene climate and cultural changes in the southwestern United States. Science 294(5540), 148-151. DOI: 10.1126/science.1062771

Proctor, C., Baker, A., Barnes, W., Gilmour, M., 2000. A thousand year speleothem proxy record of North Atlantic climate from Scotland. Clim. Dyn. 16, 815-820. DOI: 10.1007/s003820000077

Railsback, B., Liang, F., Vidal-Romaní, J., Blanche, K., Sellers, R., Vaqueiro-Rodríguez, M., Grandal-d'Anglade, A., Cheng, H., Lawrence, R., 2017. Radiometric, isotopic, and petrographic evidence of changing interglacials over the past 550,000 years from six stalagmites from the Serra do Courel in the Cordillera Cantábrica of northwestern Spain. Palaeogeogr. Palaeoclimatol. Palaeoecol. 466, 137-152. DOI: 10.1016/j.palaeo.2016.11.020

Rossi, C., Lozano, R., 2016. Hydrochemical controls on aragonite versus calcite precipitation in cave dripwaters. Geochimi. Cosmochimi. Acta 192, 70-96. DOI: 10.1016/j.gca.2016.07.021

Scroxton, N., Burns, S., Dawson, P., Rhodes, M., Brent, K., McGee, D., Heijnis, H., Gadd, P., Hantoro, W., Gagan, M., 2018. Rapid measurement of strontium in speleothems using core-scanning micro X-ray fluorescence. Chem. Geol. 487, 12-22. DOI: 10.1016/j.chemgeo.2018.04.008

Spötl, C., Fairchild, I. Tooth, A., 2005. Cave air control on dripwater geochemistry, Obir Caves (Austria): Implications for speleothem deposition in dynamically ventilated caves. Geochimi. Cosmochimi Acta 69(10), 2451-2468. DOI: 10.1016/j.gca.2004.12.009

Turgeon, S., Lundberg, J., 2001. Chronology of discontinuities and petrology of speleothems as paleoclimatic indicators of the klamath mountains, Southwest Oregon, USA. Carbonates Evaporites 16(2), 153-167. DOI: 10.1007/BF03175833

Vanghi, V., Iriarte, E., Aranburu, A., 2015. High resolution X-ray computed tomography for petrological characterization of speleothems. J. Cave Karst Stud. Natl. Speleol. Soc. Bull. 77, 75-82. DOI: 10.4311/2014ES0102

Walczak, I., Baldini, J., Baldini, L., McDermott, F., Marsden, S., Standish, C., Richards, D., Andreo, B., Slater, J., 2015. Reconstructing high-resolution climate using CT scanning of unsectioned stalagmites: A case study identifying the mid-Holocene onset of the Mediterranean climate in southern Iberia. Quat. Sci. Rev. 127, 117-128. DOI: 10.1016/j.quascirev.2015.06.013

White, W., 2006. Identification of cave minerals by Raman spectroscopy: New technology for non-destructive analysis. Int. J. Speleol. 352, 103-107. DOI: 10.5038/1827-806X.35.2.6

Wong, C., Breecker, D., 2015. Advancements in the use of speleothems as climate archives. Quat. Sci. Rev. 127, 1-18. DOI: 10.1016/j.quascirev.2015.07.019

Yadava, M., Ramesh, R., Pant, G., 2004. Past monsoon rainfall variations in peninsular India recorded in a 331-year-old speleothem. Holocene 14, 517-524. DOI: 10.1191/0959683604hl728rp

Zafra, D., 2019. Caracterización geoespeleológica de sistemas kársticos en Zapatoca Santander con fines de geoeducación y geoconservación, caso de las cavernas: El Nitro y Las Alsacias. Undergraduate thesis, Universidad Industrial de Santander, Bucaramanga, Colombia. DOI: 10.13140/RG.2.2.10891.95526/1

Zhang, J., Li, T.-Y., 2019. Seasonal and interannual variations of hydrochemical characteristics and stable isotopic compositions of drip waters in Furong Cave, southwest China based on 12 years monitoring. J. Hydrol. 572, 40-50. DOI: 10.1016/j.jhydrol.2019.02.052

Zizu, N., Schwarcz, H., Konnyer, N., Chow, T., Noseworthy, M., 2012. Macroholes in stalagmites and the search for lost water. J. Geophys. Res. 117, F03020. DOI: 10.1029/2011JF002288

Annex 1

SEM results - Sample 1: Belonging to the rock wall at the entrance to El Nitro Cavern, this is a biocritical wackstone-type limestone with the presence of terrigens, pyrite, iron oxides and malachite.

Point 1 – M1: At this point is the $CaCO_3$ composition in which calcium is the most abundant element (48.21%), this refers to the rock matrix in this case carbonate mud or micrite.

Point 2 – M1: In this, a large amount of Sulfur (39%) and Fe (34%) were found in a crystal with a subhedral shape, the associated mineral is pyrite FeS_2 and represents anoxic environments.

Point 3 – M1: At this point iron oxides can be observed, with quantitative values of Fe (49%) and O (34%) probably belonging to Hematite Fe_2O_3 or goethite generated by alteration and oxidation of the rock.

Point 4 - M1: At this point, a high concentration of the element Copper (64%) was found, indicating the presence of the hydrated copper carbonate mineral, Malachite Cu_2CO_3 (OH) 2, revealing that this marine basin received contributions of this precious metal.

Point 5 – M1: This point refers to quartz crystals ($Si0_2$) that are found in limestone rock and that belong to terrigens or continental fragments that were transported to the basin.

Point 6 - M1: This point is characterized by the high contents of Aluminum (22%) and silica (24%) to an Aluminosilicate, probably a plagioclase feldspar or some clay.

(Figure 15)

SEM Results – Sample 2: Belonging to the rock wall at the entrance to the Las Alsacias cave, it is a biomicritic packstone with iron oxides, terrigens, potassium and calcium feldspars.

Point 1 – M2: At this point, the limestone rock matrix was characterized and it was found to be composed of $CaCO_3$ and specifically the so-called biomicritic sludge.

Point 2 – M2: There is a clay mineral belonging to the Potassium aluminosilicates (14%), more specifically Potassium Feldspars such as Orthoclase ($KAlSi_3O_8$), some metal impurities such as: Fe, Al, Ti and Mg are also recorded.

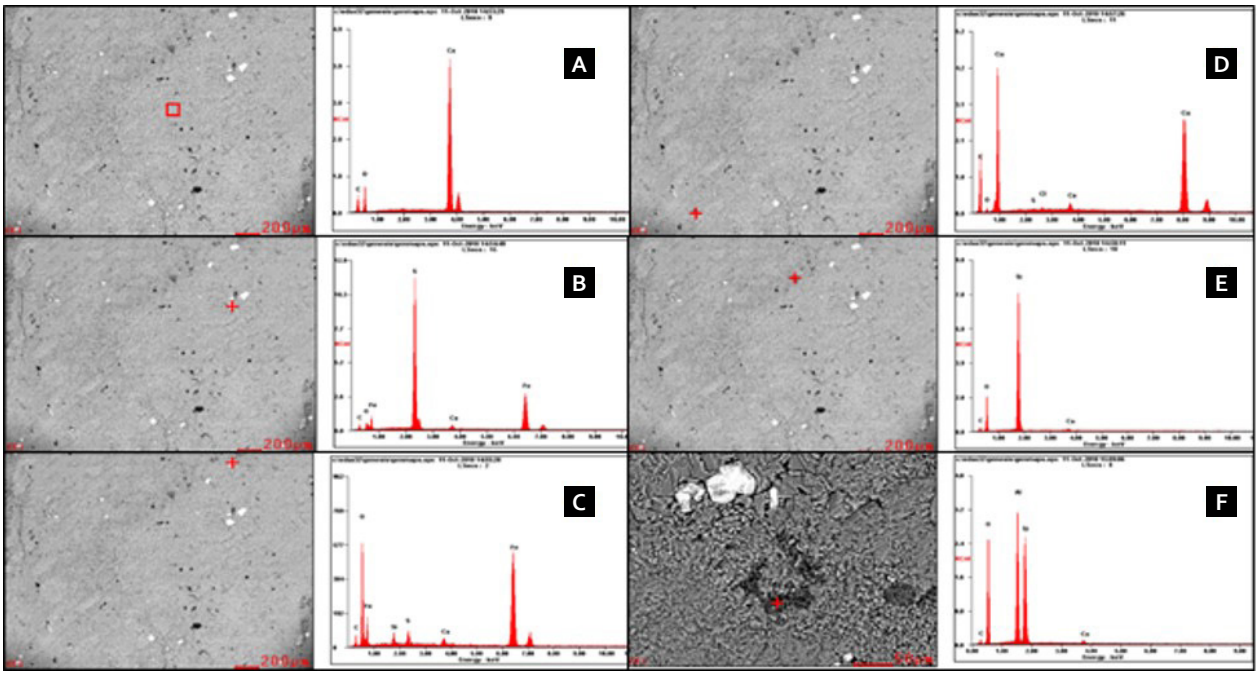

Figure 15. Sample points 1, SEM-UIS scanning electron microscope images. (A) Point 1. (B) Point 2. (C) Point 3. (D) Point 4. (E) Point 5. (F) Point 6

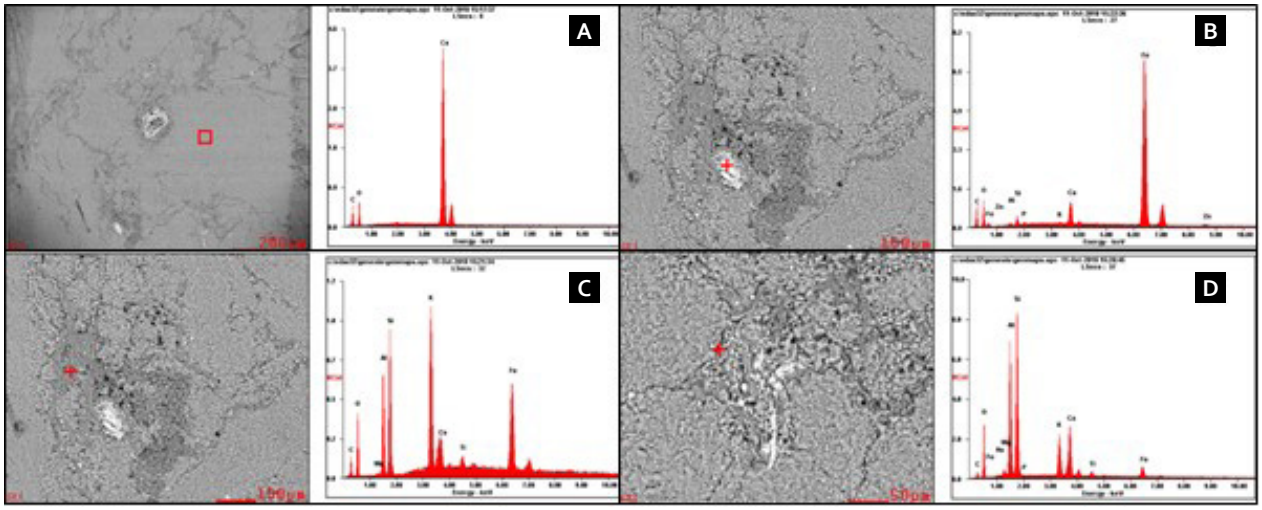

Figure 16. Points of sample 2, SEM-UIS scanning electron microscope images. (A) Point 1. (B) Point 2. (C) Point 3. (D) Point 4

Point 3 – M2: An iron oxide (Goethite - Hematite) is associated with different important metals such as: Aluminum and Zinc.

Point 4 – M2: There is an aluminosilicate of the plagioclase feldspar type, in this case calcium, with the presence of clays and different associated metals such as: Fe, Ti and Mg.

(Figure 16)

Results SEM – Sample 3: This sample belongs to crystalline parietal casts found in the "Los Diamonds" room, they are laminar castings composed of calcite, aragonite and gypsum; with the presence of some zircons between the sheets

Point 1 – M3: The majority mineral compositionally is calcite, with a calcium percentage of more than 50% representing a large part of the sample studied.

Point 2 - M3: This point studies the yellowish bands of the sample and finds that the majority element is Calcium (37%), the sample has high impurities of Phosphorus (15%) that gives it its coloration, there are also other accessory elements in smaller quantities. such as: Na, Cl, Mg, Si, S, Si, Fe and Al, which reveal an origin of the precipitate with high atmospheric pollution.

Point 3 – M3: This point shows components of (42%) of Zirconium almost half of the total composition, indicating that a saturated paleoprecipitation event in microscopic Zircons that were embedded in sheets within the casts. (Figure 17)

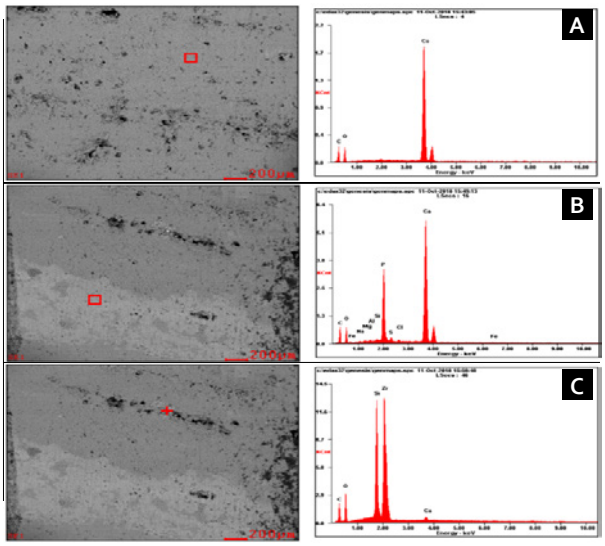

Figure 17. Points of sample 3, SEM-UIS scanning electron microscope image. (A) Point 1. (B) Point 2. (C) Point 3

Results SEM – Sample 4: This sample belongs to the same room from which stalagmite 2 was collected (last upper gallery room - second castle), Stalactite composed of calcite with different compositional impurities between its conduits, it has rhodochrosite crystals as an accessory.

Point 1 – M4: This point shows us the general composition of the sample, which mostly contains calcium carbonate $CaC0_3$.

Point 2 – M4: At this point there is a high concentration of the element Manganese (50%), which indicates that this crystal belongs to the mineral

Rhodochrosite ($MnCO_3$) or manganese carbonate, in turn large amounts of other elements and impurities are observed as accessories : Na, S, Cl, K and Ba. (Figure 18)

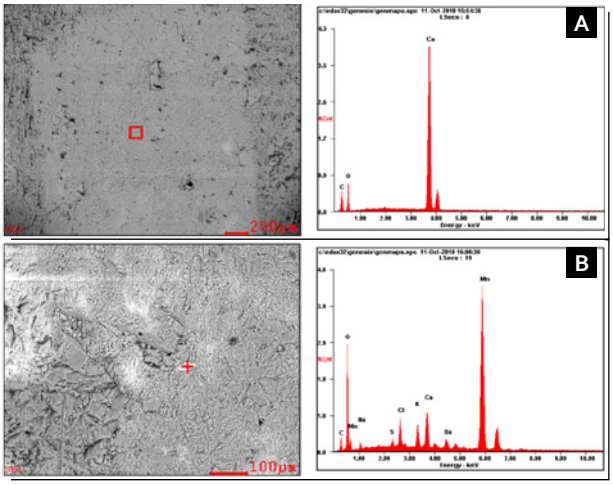

Figure 18. Points of sample 4, SEM-UIS scanning electron microscopy image. (A) Point 1. (B) Point 2